Cre-assisted Fine-mapping of Neural Circuits using Orthogonal Split Inteins

Haojiang Luan[1], Alexander Kuzin[2], Ward F. Odenwald[2], and Benjamin H. White[1,3]

[1]Laboratory of Molecular Biology, National Institute of Mental Health, NIH, Bethesda, MD 20892, USA

[2]Neural Cell-Fate Determinants Section, National Institute of Neurological Disorders and Stroke, NIH, Bethesda, MD 20892, USA

[3]Lead Contact

Running Title: Class-Lineage Intersections Using Split Cre

Correspondence to:

Benjamin White

E-mail: benjaminwhite@mail.nih.gov

Summary:

Genetic methods for targeting small numbers of neurons of a specific type are critical for mapping the brain circuits underlying behavior. Existing methods can provide exquisite targeting precision in favorable cases, but for many cases alternative techniques will be required. Here, we introduce a new step-wise combinatorial method for sequentially refining neuronal targeting: Depending on the restriction achieved at the first step, a second step can be easily implemented to further refine expression. For both steps, the new method relies on two independent intersections. The primary intersection targets neurons based on their developmental origins (i.e. lineage) and terminal identities, while the second intersection limits the number of lineages represented in the primary intersection by selecting lineages with overlapping activity of two distinct enhancers during neurogenesis. Our method relies critically on two libraries of 134 transgenic fly lines that express fragments of a split Cre recombinase under the control of distinct neuroblast enhancers. The split Cre fragments are fused to non-interacting pairs of split inteins, which ensure reconstitution of full-length and active Cre when all fragments are expressed in the same cell. Our split Cre system, together with its open source libraries, represent off-the-shelf components that should facilitate the targeting and characterization of brain circuits in *Drosophila*. Our methodology may also prove useful in other genetic model organisms.

Keywords:

Circuit mapping, neuronal lineage, neuroblast, binary expression system, Gal4-UAS, behavior, proboscis extension, dopamine, *Drosophila*

Introduction:

An essential step in mapping brain circuits is identifying the function of the individual neurons that comprise them. This is commonly achieved by manipulating neuronal function using effectors encoded by transgenes whose expression is targeted to small subsets of cells using the regulatory elements of neutrally-expressed genes (Gohl et al., 2017; Luo et al., 2018). While it has proved relatively easy to target large groups of neurons for cellular manipulation by this means in genetic model organisms using binary expression systems, such as the Cre-lox system of mice or the Gal4-UAS system of fruit flies, highly-specific targeting of neurons requires combinatorial methods. Genetic combinatorial methods typically use either the regulatory elements of two or more neurally-expressed genes, or exploit stochastic events to limit transgene targeting to a subpopulation of a larger group of neurons. In fruit flies, both types of method are capable of targeting single cells or cell types under optimal conditions (Aso et al., 2014; Flood et al., 2013; Gordon and Scott, 2009; Luan et al., 2012; Shang et al., 2008). However, both approaches have limitations: stochastic methods are, by nature, poorly reproducible, while combinatorial methods are labor-intensive, often requiring the characterization of many neurally active enhancer elements (Dionne et al., 2018; Tirian et al., 2017). Simpler methods of targeting small populations of brain cells are therefore desirable in the effort to comprehensively map neural function.

An attractive approach to increase the specificity of neuronal targeting is to identify neurons based not only on the genes they express in the terminally differentiated state (i.e. terminal effector genes, TEG), but also on their developmental history (Awasaki et al., 2014; Dymecki et al., 2010; Huang, 2014). Most neuronal lineages produce diverse neuron types, and while some striking correspondences have been found (Lacin et al., 2019), lineage identity, in general,

correlates poorly with neuronal identity as defined by gene expression (Hobert et al., 2016; Zeng and Sanes, 2017). Conversely, gene expression is often correlated across neurons that differ in identity as defined by their function, morphology, and neuroanatomical location (Hobert, 2016; Hobert and Kratsios, 2019). This is because neuronal identities are defined not by single genes, but by the expression of often overlapping batteries of TEGs. An intersection of lineage with the expression of a specific TEG may thus, in general, include fewer neurons than an intersection of the expression patterns of two TEGs. In addition, because neurons from a given lineage typically remain regionally localized, intersections made using lineage information will tend to restrict neuronal targeting anatomically.

Recombinase-based intersectional methods that combine information about lineage and cell type have been developed in both mice and fruit flies and have been shown to substantially restrict targeting to cell groups of interest (Brust et al., 2014; Ren et al., 2016). However, the use of such methods has remained largely limited to specific cases—in mice, sublineages of brainstem serotonergic neurons (Okaty et al., 2015), and in flies, subtypes of Type II transit-amplifying neural stem cells (i.e. neuroblasts, NBs) of the central brain (Ren et al., 2018; Ren et al., 2017). This is because of the paucity of lineage-restricted enhancers. Just as there are few TEG enhancers that are active in small numbers of mature neurons, there are also few identified enhancers that exhibit lineage-specific activity. In the fly, a systematic analysis of some 5000 neural enhancer domains identified 761 with activity in embryonic NBs, but 99 of these expressed in most or all lineages (Manning et al., 2012). A separate analysis indicates that the remainder are at best active in 5-20 lineages (Awasaki et al., 2014). The routine use of lineage-cell type intersections for neural circuit mapping will thus require more refined methods of isolating neuronal lineages or sub-lineages.

To achieve such lineage refinement, we introduce here a combinatorial method analogous to the Split Gal4 technique used to restrict neuronal targeting to the intersection of two TEG expression patterns (Luan et al., 2006). We restrict reconstitution of a Split Cre recombinase to the expression patterns of two independent NB-active enhancers (i.e. NBEs). Only NBs in which both enhancers are active thus make full-length Cre. Cre is then used to selectively promote activity of the Gal4 transcription factor—expressed under the control of a TEG enhancer—in the mature progeny of these NBs, thus implementing a second intersection. Our method (i.e. "Split Cre-assisted Restriction of Cell Class-Lineage Intersections," or SpaRCLIn) generalizes the capabilities of the CLIn technique introduced by Ren et al. (Ren et al., 2016) by expanding the range of possible intersections to most *Drosophila* lineages while maintaining compatibility with all existing *Drosophila* Gal4 driver lines. To facilitate SpaRCLIn's use, we have generated a variety of tools, including two libraries of transgenic fly lines, each of which expresses distinct Split Cre components under the control of 134 different NBEs. We characterize the efficacy of these SpaRCLIn reagents and provide examples of their use in restricted neuronal targeting and circuit-mapping.

Results

Development of Bipartite and Tripartite Split Cre Recombinases

SpaRCLIn was developed to refine the expression pattern of a Gal4 driver using the basic strategy shown in Figure 1. In common with other existing methodologies, SpaRCLIn uses a recombinase (i.e. Cre) to excise an otherwise ubiquitously expressed construct encoding Gal80, a suppressor of the Gal4 transcription factor (Fig. 1A-B). As in the CLIn technique, recombinase expression—and thus the excision of Gal80—occurs only in targeted NBs, rendering the progeny of these NBs permissive to Gal4 activity (Fig. 1C). Those progeny that lie within the expression pattern of the Gal4 driver will be competent to drive UAS-reporters and effectors, such as UAS-GFP. In the SpaRCLIn technique, distinct NBEs are used to express components of a bipartite Split Cre molecule in restricted subsets of NBs. In lineages of these NBs that contain mature neurons within the Gal4 expression pattern, Gal4 will be active. This population of neurons can be additionally parsed using a tripartite Split Cre to further restrict the subset of NBs that make active Cre (Fig. 1D).

Although most recombinase-based expression systems in *Drosophila* , such as MARCM (Lee and Luo, 1999), Flp-out Gal80 (Gordon and Scott, 2009), and FINGR (Bohm et al., 2010) have preferentially used the Flp recombinase for Gal80 excision, we selected Cre for use in SpaRCLIn because of its demonstrated ability to retain high activity in a variety of bipartite forms (Hirrlinger et al., 2009; Jullien et al., 2003; Kawano et al., 2016; Kennedy et al., 2010; Rajaee and Ow, 2017). Although Cre activity has been reported to be toxic in *Drosophila* when chronically expressed at high levels (Heidmann and Lehner, 2001; Nern et al., 2011), it has previously been used in NBs without apparent adverse effects (Awasaki et al., 2014; Hampel et

al., 2011; Ren et al., 2016). Because our system requires use of a tripartite Cre to achieve the most refined targeting it was also desirable to use a method of splitting Cre that would permit reconstitution of the intact molecule to obtain the highest activity levels. Split inteins, which are capable of autocatalytically joining two proteins to which they are fused, are well-suited to this purpose and distinct split inteins have been previously shown to support reconstitution of recombinase activity from complementary Cre fragments fused to them (Ge et al., 2016; Han et al., 2013; Hermann et al., 2014; Wang et al., 2012). Figure 1E shows the primary structure of Cre, indicating the location of the breakpoints (green highlight) at which we introduced split intein moieties into the molecule. These breakpoints separate the amino acid residues in the primary structure that form the DNA-binding sites (blue) and the active site (yellow highlight), thus insuring that none of the fragments retains catalytic activity. Two Split Cre fragments, Cre_{AB} and Cre_{C}, were generated by the breakpoint between amino acids P250 and S251 to implement the bipartite Split Cre system (Fig. 1F, G), while dividing the Cre_{AB} fragment at the breakpoint between amino acids D109 and S110 was used to create two further fragments (i.e. Cre_{A} and Cre_{B}) which together with Cre_{C} form the basis of the tripartite Split Cre system (Fig. 1H, I). The split intein pairs used to generate these fragments, gp41-1 and NrdJ-1, were chosen based on their trans-splicing efficiency and their lack of cross-reactivity (Carvajal-Vallejos et al., 2012). The latter criterion was critical for avoiding the generation of unproductive fusion products of the Cre fragments.

After confirming the ability of the bi- and tripartite constructs to reconstitute Cre activity when co-expressed in transfected S2 cells (data not shown), we used them to generate transgenic fly lines in which they were expressed in patterns dictated by individual enhancers that exhibited activity in neuroblasts. Most of the NBEs selected for this purpose (Supplementary Table 1)

were taken from the large collection of enhancer fragments with fully defined sequences created by the Rubin lab (Manning et al., 2012; Pfeiffer et al., 2008), with the remainder characterized as indicated. A total of 134 NBEs were used to make two libraries of transgenic fly lines, one expressing the Cre_B fragment under the control of each of the 134 NBEs and the other similarly expressing the Cre_C fragment. These lines thus collectively express Cre_B and Cre_C in a large number of distinct and often overlapping subsets of NBs (Figure 1—figure supplement 1). However, because the 134 enhancers are also typically active in mature neurons, the production of full-length Cre is not necessarily restricted to NBs (Jenett et al., 2012).

To ensure NB-specific reconstitution of Cre activity, we placed the Cre_A and Cre_{AB} fragments under the control of a compound enhancer formed by fusing individual enhancer elements of the NB-specific genes, *deadpan (dpn)* and *nervous fingers-1 (nerfin-1*; see Materials and Methods). This synthetic *dpn-nerfin-1* enhancer (i.e. DNE) combines the complementary temporal characteristics of both component enhancers, maintaining strong, broad, and specific activity throughout embryonic neurogenesis (Figure 1—figure supplement 2). Use of the DNE thus ensured that full-length, active Cre would be generated only in NBs where expression of the Cre fragments overlapped, and not in fully-differentiated neurons (Fig. 1G, I). This enhancer also expresses in most of the NBs that give rise to the *Drosophila* CNS with the exception of those found in the late-developing optic lobes, and thus guarantees substantial coverage of the mature neurons found within the expression patterns of Gal4 lines.

To detect activity of the Split Cre constructs *in vivo*, we created transgenic flies carrying a reporter construct in which the floxed Gal80 gene, the expression of which is driven by a

ubiquitously active Actin 5C promoter, is followed by the gene encoding the red fluorescent protein, tdTomato (Fig. 1J). Expression of tdTomato from this construct, which we call Cre80Tom, thus identifies neurons in which Gal80 has been excised, as illustrated by the expression patterns shown in Figure 1K and L. These patterns in the central nervous systems (CNS) of third instar larvae were generated by the bipartite system using the DNE-Cre_{AB} fragment and Cre_C expressed under the control of two different neuroblast enhancers (NBE_{43H02} and NBE_{44F03}). The expression patterns include not only the NBs in which Cre activity is reconstituted, but also the progeny of these NBs, since tdTomato expression is activated in all cells born within these lineages after Gal80 is excised. Although the expression patterns differ in the two cases, they share a small number of common NB lineages as is revealed by application of the tripartite Cre system using the NBE_{44F03} and NBE_{43H02} enhancers to drive Cre_B and Cre_C, respectively, together with DNE-Cre_A (Fig. 1M). Expression in this case is limited to approximately three bilateral lineages in the ventral nerve cord (VNC) and two in the brain. These examples illustrate how the bi- and tripartite Split Cre constructs selectively reconstitute Cre activity in NBs targeted by individual NBEs, and demonstrate that the tripartite Split Cre system can be used to restrict Cre activity to only those NBs in which two distinct NBEs are active. The tripartite system thus represents an intersectional method for restricting Cre activity to subsets of NBs. The progeny of these NBs that are generated after Cre activation will not only express the reporter tdTomato, but will also fail to express the Gal80 transgene, thus permitting Gal4 to function.

Using the Bipartite and Tripartite Cre Systems to Restrict Expression of TH-Gal4

The selective disinhibition of Gal4 activity in targeted lineages permits UAS-transgenes to be expressed in cells of those lineages whenever they lie within the expression pattern of a Gal4 driver. This allows targeted lineages to be parsed according to the properties of the mature neurons to which they give rise using cell-type specific Gal4 drivers. Such so-called "cell class-lineage intersections" have been previously performed to identify subsets of neurons generated by Type II NBs of the *Drosophila* brain, which can be selectively targeted using a Type II-specific enhancer (Ren et al., 2016; Ren et al., 2018; Ren et al., 2017). Among the neurons generated by Type II NBs are several populations of dopaminergic neurons, identified by a Tyrosine Hydroxylase-specific Gal4 driver (TH-Gal4). Dopaminergic neurons are of considerable interest because of their roles in a variety of important neurobiological processes, including learning, sleep, and locomotion (for review see Kasture et al., 2018). The approximately 120-130 dopaminergic neurons in the *Drosophila* CNS are produced by diverse NBs and numerous reagents have been generated to selectively target them (Aso et al., 2014; Friggi-Grelin et al., 2003; Xie et al., 2018).

As a first test of the SpaRCLIn system, we therefore asked whether it could restrict expression of the TH-Gal4 driver (Fig. 2A) to small numbers of distinct dopaminergic neurons based on their different lineages of origin. Using a small subset of the NBE-Cre_C lines in combination with DNE-Cre_{AB}, we examined the expression patterns produced by intersection with TH-Gal4. The expression patterns produced by these intersections were noticeably reduced compared with the full pattern of the TH-Gal4 driver, but they typically still contained 10's of dopaminergic neurons distributed broadly across the neuraxis (Fig. 2B-C). In cases where the expression patterns produced by the bipartite crosses shared a neuron (Fig. 2B-C, arrows), combining the relevant NBEs using the tripartite system succeeded in isolating these neurons from most others

in the two original crosses (Fig. 2D). In general, restricting NB expression using the tripartite system—by pairing the NBE-Cre_C constructs with NBE-Cre_B constructs made with different enhancers—produced significantly reduced expression patterns, sometimes consisting of one to two cells or bilateral cell pairs (Fig. 2D-H).

The expression patterns from 14 NBE-Cre_C∩NBE-Cre_B intersections—produced by combining 15 distinct NBEs—were analyzed in detail to quantify both the average number of dopaminergic neurons and the stereotypy of expression for each intersection (Fig. 2I). We found that the average number of labeled neurons per preparation did not exceed 8.5 (±3.8, n=16) for any intersection and was less than 4.3 (±2.3, n=17) for two-thirds of them. This sparseness of expression suggests that the NBEs tested do not overlap extensively in their NB expression patterns. Stereotypy of expression was also generally present despite considerable variability. Only in one extreme case, did there appear to be a complete absence of stereotypy, with all CNS preparations that had expression displaying a distinct pattern (Figure 2—figure supplement 1). For all other intersections, at least one principal neuron was found that was shared by multiple preparations, based on cell position and morphology (Fig. 2I, black bars). For over half of the intersections, this principal common neuron was shared by 50% or more of preparations. In most cases, other neurons were also found, though preparations containing only such neurons typically occurred at lower frequency (Fig. 2I, gray bars). Consistent with this variability of expression, neurons that recurred across preparations were not necessarily found in the same combinations (Fig. 2—figure supplement 2).

The sparseness of labeling combined with the variability of expression likely accounts for why half of the intersections yielded at least one preparation without any expression. Interestingly,

four of the seven intersections that yielded preparations devoid of expression shared an enhancer (R14E10), suggesting that particular enhancers may strongly influence the extent of labeling. Variability of labeling also appeared to be enhancer-dependent in that use of the same enhancer (i.e. R17A10) to drive both Cre_B and Cre_C components did not necessarily reduce stochasticity. Indeed, although all preparations that had expression shared a common identifiable neuron in this case (Fig. 2I), their expression in other neurons varied considerably. A possible source of this variability of expression is weak NBE activity that results in lowered expression of Cre components and consequently more sporadic reconstitution of Cre activity. More work will be required to examine this hypothesis. Regardless, our results demonstrate SpaRCLIn's ability to substantially restrict expression of a Gal4 driver with sufficient stereotypy in single neurons to be useful for the neuronal manipulations employed in neural circuit mapping.

Functional circuit-mapping using SpaRCLIn

To examine SpaRCLIn's efficacy for circuit mapping, we used it to identify neural substrates of proboscis extension (PE), a motor pattern normally elicited by gustatory stimuli, but also by the hormone Bursicon in newly eclosed flies (Peabody et al., 2009). Robust PE can be readily induced even in older flies using a driver (rk^{pan}-Gal4) that selectively expresses in Bursicon-responsive neurons (Video 1, Fig. 3A, B Diao and White, 2012). Expressing the heat-sensitive ion channel UAS-dTrpA1 under the control of this driver, we performed an initial ("Step 1") screen of the Cre_C library using the bipartite SpaRCLIn system (Figure 3—figure supplement 1A). In this screen, crosses were conducted between each NBE-Cre_C line and a line that combined all other components, including Cre80Tom, DNE-Cre_{AB}, rk^{pan}-Gal4, and UAS-dTrpA1. To facilitate visualization of neurons within the resulting expression pattern without

requiring additional genomic insertions, we used a dual expression construct (Cre80Tom- GFP) that contained actin^Gal80^myr-tdTomato and a 10XUAS-mCD8GFP reporter (Figure 3—figure supplement 2). Progeny were videorecorded in small chambers on a temperature-controlled plate and assayed for heat-induced PE. Interestingly, several different PE phenotypes were apparent, but only those that involved full extension of the proboscis could be reliably scored under our assay conditions and we therefore focused on the latter. Applying this criterion, we identified 23 NBE-Cre_C∩DNE-Cre_{AB} intersections for which UAS-dTrpA1 activation reliably induced robust PE in greater than 50% of the progeny. The expression patterns resulting from these $Cre_{AB∩C}$∩rk^{pan}-Gal4 (i.e. Step 1) intersections, examined using a UAS-GFP reporter, were clearly restricted relative to rk^{pan}-Gal4 expression (Fig. 3C-D), but they were insufficiently sparse to readily identify the neurons—or population of neurons—responsible for inducing the PE motor pattern.

Taking advantage of SpaRCLIn's ability to further restrict expression, we used the tripartite system to carry out a second ("Step 2") screen in which the 23 identified NBE-Cre_C components were combined pairwise with NBE-Cre_B components made using the same 23 enhancers (Figure 3—Supplement 1B). The latter were selected from the NBE-Cre_B library and crosses were made that combined distinct NBE-Cre_B and NBE-Cre_C components with DNE-Cre_A, rk^{pan}-Gal4, and Cre80Tom-GFP. These Step 2 crosses resulted in $Cre_{A∩B∩C}$ ∩ rk^{pan}-Gal4 intersections that were assayed for PE as before. Of the approximately 70 intersections tested, 11 yielded PE phenotypes in greater than 50% of flies. The phenotype observed was typically less sustained than that produced by activation of the full rk^{pan}-Gal4 expression pattern in that activation typically caused rhythmic, rather than tonic, extension of the proboscis, which after prolonged heating often transitioned to lifting of the rostrum rather than full extension (Video 2; Fig. 3E).

The rk^{pan}-Gal4 expression patterns in flies exhibiting this phenotype were substantially reduced for many of the intersections tested and they consistently included particular neurons in the subesophageal zone (SEZ) that were characterized by somata near the saddle, broad arbors along the superior gnathal ganglion (GNG), and axons that extended medially before turning, with one branch coursing down each side of the midline and then turning laterally along the medial-inferior edges of the GNG (Video 3). Two closely apposed neurons of this type were observed, sometimes as bilateral pairs (Fig. 3F), and sometimes on only one side (Fig. 3G). These neurons, which we call the PE^{rk} neurons, were notably prominent in the 16H11-Cre_B∩44F09-Cre_C intersection, where they constituted the entire expression pattern of 16 animals (n=78 total), all of which exhibited PE induction upon heating. Indeed, all 36 animals from this intersection that tested positive for the PE phenotype and were successfully dissected showed expression in the PE^{rk} neurons, while none of the animals (n=38) that tested negative had such expression (Fig. 3I). Most of the latter, in fact, had little to no expression. Similar results were obtained with a second intersection (44F09-Cre_B∩10G07-Cre_C). All 19 animals that exhibited induced PE in this intersection had expression in the PE^{rk} neurons, and in three animals these were the only neurons present. A third intersection that yielded the PE phenotype in all animals likewise showed consistent expression in the PE^{rk} neurons, but the correlation between the PE phenotype and expression in these neurons was somewhat less readily established because of expression in other neurons (5.6 ± 1.8; n=14 preparations; Fig. 3—figure supplement 3).

FRTerminator: a self-excising DNE-Cre_{AB} to facilitate fine-mapping in Step 1 screens

The above examples demonstrate that SpaRCLIn can be used to rationally parse the expression patterns of Gal4 drivers using the workflow shown in Fig. 3—figure supplement 1. One challenge to using this system, however, is the large number of transgenes required to implement

it. This is especially true for Step 2 screening with the tripartite system. To mitigate this burden, we have created several reagents that will facilitate use of the system. In addition to the Cre80Tom-GFP construct described above, we have developed other dicistronic constructs to facilitate manipulating neuronal activity in SpaRCLIn screens (see Key Resources Table). These include constructs and fly lines for Cre80-Kir2.1 and Cre80-dTrpA1. In addition, we have developed an alternate Step 1 strategy that may avert the need for Step 2 screening in favorable cases.

The alternate strategy uses a transiently expressed DNE-Cre_{AB} designed to be active only during early stages of neurogenesis. This construct, which we call "FRTerminator," is self-excising in that it is flanked by Flp Recombination Target (FRT) sites and encodes a Flp recombinase gene that is co-expressed with Cre_{AB} (Fig. 4A). Upon expression under control of the DNE enhancer, this construct will remove the Cre_{AB} gene and thus limit its expression to early (embryonic) neuroblasts (Fig. 4B). Cre_{AB} will thus be available to reconstitute Cre activity only with complimentary Cre_C fragments that are also expressed at this time. Cre_Cs whose expression is driven by NBEs that become active only after the elimination of Cre_{AB} from neuroblasts, will not lead to the generation of Gal4-competent neurons. Expression patterns resulting from the combination of FRTerminator with NBE-Cre_Cs will thus, in general, be reduced relative to those produced by DNE-Cre_{AB} (Fig. 4C,D).

To determine whether the FRTerminator might therefore expedite parsing of Gal4 expression using the SpaRCLIn system, we repeated selected crosses from the rk^{pan}-Gal4 Step 1 screen described above. We focused on the 23 NBE-Cre_C lines that yielded flies with PE phenotypes, combining each with the FRTerminator, rk^{pan}-Gal4 and Cre80-GFP. Progeny were tested for PE

upon dTrpA1 activation. We found that three NBE-Cre_C lines (44F09, 57B09, and 14E10) produced progeny with PE phenotypes at frequencies ranging from 9-17%. Although these frequencies were considerably lower than those obtained using DNE-Cre_{AB}, the resulting expression patterns were substantially sparser compared with those of progeny from DNE-Cre_{AB} crosses (Fig. 4E, F). All animals examined that had PE phenotypes also included in their expression patterns the PE^{rk} neurons (n=40). In contrast, only one of the animals examined that lacked the phenotype had these neurons (n=39). A strong correlation between PE and the presence of the PE^{rk} neurons was thus observed, again permitting the conclusion that these neurons are substrates for the behavioral phenotype. We conclude that FRTerminator-based Step 1 screens may serve as a useful shortcut to serial Step 1 and Step 2 screens for restricting Gal4 expression and identifying functionally important neuronal subsets.

Discussion

The SpaRCLIn system introduced here permits the refined targeting of neurons within a group of interest based on both their developmental origins and their patterns of gene expression in the terminally differentiated state. By permitting the combinatorial targeting of many, if not most, of the neuroblasts that generate the mature CNS, the SpaRCLIn system provides end-users with a comprehensive, "off-the-shelf" set of reagents for systematically isolating and characterizing the anatomy and function of specific neurons. The reagents that we have created include extensive lineage-selective Split Cre lines for bipartite (Step 1) and tripartite (Step 2) neuronal screens, in addition to a range of tools that facilitate application of the system. Dual effector and reporter constructs reduce the number of transgenes required to implement the system, and a self-terminating Split Cre component (i.e. FRTerminator) can be used to expedite screening in favorable circumstances. The system is compatible with existing Gal4 driver lines and the examples provided here indicate that it is capable of routinely parsing Gal4 expression patterns into subsets of neurons numbering in the single digits.

Utility of SpaRCLIn to circuit mapping

Our use of SpaRCLIn to identify the RK-expressing neurons that trigger robust proboscis extension demonstrates SpaRCLIn's ability to systematically parse a neuronal group and identify the functionally relevant subset. Just over 200 crosses—134 crosses for the Step 1 screen of NBE-Cre_C lines and 70 NBE-$Cre_{B\cap C}$ Step 2 crosses—were required to identify two pairs of command-like neurons capable of inducing PE upon activation (i.e. the PE^{rk} neurons). Importantly, our Step 2 screen, although it included only 70 of the 253 possible intersections, was nevertheless redundant in that the command-like neurons were prominent in the expression

patterns of numerous independent Step 2 intersections and were readily correlated with PE induction in three that produced particularly reduced expression patterns. In the intersection with the sparsest expression, the two pairs of PE-inducing neurons often comprised the entire observable pattern in flies that had the PE phenotype, illustrating the extreme reduction in expression achievable with SpaRCLIn. The demonstration that the PE^{rk} neurons can be isolated in single crosses using the FRTerminator indicates that this reduction in expression can be attained without the labor of Step 2 screening. However, the lower frequency of the PE phenotype in FRTerminator crosses in our example also suggests that FRTerminator-based screens may require testing more animals for each intersection than a standard Step 1 screen in order to reliably identify positives.

Activation of the PE^{rk} neurons elicits rhythmic proboscis extension, rather than the tonic PE elicited by activation of all rk^{pan}-Gal4 neurons. This suggests that additional RK-expressing neurons—perhaps lacking command capability—modulate the effects of activating the PE^{rk} neurons. Based on their induction of rhythmic extension and their apparent lack of a projection to the proboscis muscles, we conjecture that the PE^{rk} neurons identified here are not motor neurons, the activation of which results in tonic and often partial PE (Gordon and Scott, 2009; Schwarz et al., 2017). Similarly, the anatomy of the PE^{rk} neurons differs from that of other identified neurons that can drive PE when activated, including second-order projection neurons (Kain and Dahanukar, 2015), modulatory neurons (Marella et al., 2012), and a local SEZ interneuron called the Fdg-neuron (Flood et al., 2013). Like the Fdg-neuron, however, the neurons identified here seem to function in a premotor capacity, perhaps as part of the central pattern generator for PE that regulates fly feeding (Itskov et al., 2014). Further work will be required to determine the

precise role of the PE^{rk} neurons in the feeding circuitry and their relationship to other identified neurons involved in PE.

It also remains to be determined whether activation of both PE^{rk} neurons is required to induce the PE phenotype. Indeed, from the standpoint of the efficacy of the SpaRCLIn system it is important to ask why SpaRCLIn failed to separate these two pairs of neurons. The similarity of the two PE^{rk} neurons in both soma position and projection pattern is consistent with their being part of the same lineage. Such neurons will necessarily be more difficult to parse using SpaRCLIn, which can separate neurons within the same lineage only based on their birth order. What would be required to do so is having two NBEs that are active in the same lineage but at different times so that they separate earlier- from later-born neurons. Such NBEs, by generating Cre only in older neuroblasts, will generate sublineages of Gal4-competent neurons. Although many of the NBE's used to make our Cre_B and Cre_C libraries clearly generate such sublineages—based on the patterns shown in Fig. 1—Supplemental Figure 1—it is doubtful that that they cover more than a fraction of all temporal windows of neurogenesis in all neuronal lineages. A method for systematically isolating sublineages of later born neurons using SpaRCLIn may become possible if neuroblast-specific enhancers can be found that are selectively active at later stages of neurogenesis. These could then be used in lieu of the DNE used here. Candidates for such enhancers are those that determine expression of the so-called "temporal transcription factors" that regulate the progressive divisions of many neuroblasts (Doe, 2017).

Stochasticity of SpaRCLIN expression

Although stochasticity is not an uncommon feature of many expression systems (Bohm et al., 2010; Tastekin and Louis, 2017), the variability of expression generated by SpaRCLIn was

notable. Even for intersections that reliably produce very similar expression across animals, it is not common to get exactly the same pattern twice. The infidelity of expression may derive, at least in part, from intrinsic stochasticity of NBE activity, but the strength and/or temporal properties of NBE activity are other likely factors. Further work would be required to identify the sources of variable expression within the system. However the observed stochasticity is not a disadvantage for circuit-mapping applications, as illustrated by the examples presented here. By providing partially "randomized" expression patterns, SpaRCLIn permits causative relationships to be inferred between groups of manipulated neurons and the effects produced by their manipulation (Jazayeri and Afraz, 2017). Such randomization has been commonly exploited in so-called "Flp-out" methods that rely on stochastically induced recombinase activity to remove an FRT-flanked gene or transcription stop cassette (Flood et al., 2013; Gordon and Scott, 2009; Kain and Dahanukar, 2015). This logic is naturally implemented in SpaRCLIn, but because randomness of expression is considerably more constrained than that observed in systems that rely on completely stochastic methods, and because the size of the expression patterns is typically small, correlations can be readily established.

One consequence of SpaRCLIn's stochasticity that must be considered in circuit mapping applications, however, is the lowered frequency of bilateral labeling. Most neurons occur as members of bilateral pairs and we observed numerous instances in which SpaRCLIn-derived expression patterns contained only a single member of each pair in a given preparation—presumably due to the variable success of Gal80 excision in both NBs giving rise to the pair. The reduced bilateral representation of neurons may likewise reduce the frequency of phenotypes observed as a consequence of a particular manipulation if, for example, both neurons in a pair must be affected to produce a phenotype. This is often the case for suppression of function,

where both neurons in the pair must be inhibited. It is therefore possible that SpaRCLIn will be most effective in applications that involve neuronal activation where unilateral manipulations are often sufficient to generate an effect as they are for proboscis extension.

Other considerations in the use of SpaRCLIn

The ability of SpaRCLIn to isolate a given set of neurons of interest in a Gal4 pattern depends critically on the extent to which the various Split Cre components are expressed in the neuroblast lineages of the fly. This will be determined both by the breadth of NB expression of the DNE enhancer used here to delimit Cre activity and by the collective coverage of NB expression provided by the NBEs represented in the libraries of Split Cre_B and Cre_C lines. Our analysis of 3^{rd} instar larval expression in DNE∩NBE intersections (Figure 1—figure supplement1 and data not shown) indicates that many, if not most, NB lineages of the ventral nerve cord and central brain are likely represented within the libraries. Indeed, many lineages are clearly multiply represented in that different intersections repeatedly isolated the same neurons (e.g. the PE^{rk} neurons) for both the rk^{pan}-Gal4 and TH-Gal4 drivers. It is less clear, however, that all members of each lineage are represented as not all NBE's are active during early NB divisions. This is evident from the restriction in NB expression observed when the FRTerminator construct is used, since this construct acts by eliminating lineages or sublineages in which Cre activity is initiated sometime after neurogenesis has begun. It is also clear that the DNE does not express efficiently in NB lineages in the optic lobe (data not shown). To extend the capability of the system to include these lineages will require either the development of a more general neuroblast-specific enhancer or augmenting the system to include an enhancer that specifically targets optic lobe neuroblasts.

The effectiveness of SpaRCLIn also depends critically on the success of Cre reconstitution by the system, which is effected by two pairs of split inteins (Shah and Muir, 2011, 2014). These trans-splicing protein fragments function naturally in protein religation and are an emerging technology for use in transgenic animals (Hermann et al., 2014; Wang et al., 2018; Wang et al., 2012). Their advantages are that they lend themselves readily to intersectional methods, are genetically encoded, and in numerous cases display rapid reaction kinetics and low cross-reactivity. A disadvantage, on which some recent progress has been made (Stevens et al., 2017), is that most split inteins require specific flanking amino acid residues in the proteins to which they are fused, in particular a cysteine or serine residue immediately downstream of the N-intein. We were able to create self-ligating split Cre fragments capable of reconstituting full-length, active Cre enzyme in *Drosophila* NBs by choosing breakpoints in the Cre sequence preceded by a serine residue—the native condition of the NrdJ-1 and gp41-1 split inteins used here (Carvajal-Vallejos et al., 2012). Orthogonal (i.e. non-interacting) split inteins thus represent attractive tools for reconstituting the function of multiply split proteins, a methodology that should be applicable in other model organisms.

Conclusions and Future Development

Although sophisticated methods for neuronal targeting have been a hallmark of neurobiological studies on the fly, and single cell manipulations are being leveraged in a growing number of cases to elucidate *Drosophila* brain circuits, targeting every cell in the fly CNS remains an aspirational goal. Recent progress towards this goal has been made using the Split Gal4 system (Dionne et al., 2018; Tirian et al., 2017), and innovative methods continue to be developed using emerging tools (Garcia-Marques et al., 2019). An advantage of SpaRCLIn is that it represents a

relatively small set of stand-alone reagents for high-specificity neuronal targeting that can be used with the many existing components of the Gal4-UAS system. Importantly, SpaRCLIn also represents an open resource that can readily be augmented by end-users. As methods improve for rationally identifying NB lineages based on gene expression and enhancer activity, the existing SpaRCLIn libraries can be supplemented with lines that together permit the selective targeting of an increasing number of neuroblast lineages. By combining these libraries with an optimized set of Gal4 drivers that express in distinct subsets of brain cells (distinguished, for example, by transcription factor expression), one can imagine having a set of 3 libraries that in combination can selectively target most neurons in CNS.

Author Contributions:

Conceptualization, H.L., B.H.W.; Methodology, H.L., B.H.W.; Software ; Formal Analysis,; Investigation, H.L., A.K., Resources, A.K., W.F.O.; Writing, Original Draft, H.L.; Writing, Review & Editing, H.L., B.H.W., W.F.O; Visualization, H.L, B.H.W.; Supervision, B.H.W., W.F.O, and H.L.; Funding Acquisition, B.H.W., W.F.O.

Acknowledgements:

We thank Matthew Roberts, Andrew Laczarchik, and Ana Cardenas for technical help in generating the NBE-Split Cre lines described in this study. We also thank Sean Sweeney, David Anderson, and Jermaine Ross for plasmid DNA; Paul Garrity and James Kennison for fly lines; and Kiichi Watanabe for sequence details regarding the *otd* Gateway entry clone. This work was supported by the Intramural Research Programs of the National Institute of Mental Health (ZIA-MH002800, BHW) and the National Institute of Neurological Disease and Stroke (ZIA-NS002820-26). We further thank the Bloomington Drosophila Stock Center (NIH P40OD018537) for many of the fly stocks used in this study, and members of the White lab for insightful comments on the manuscript.

Competing Interests:

The authors declare no competing interests.

Figure Legends

Figure 1. Restriction of NB targeting using split Cre components fused to split inteins

(A-D) Components and genetic logic of the SpaRCLIn system. **A**) A Gal4 driver that drives expression of UAS-transgenes, such as UAS-GFP, in a specific pattern of cells within the CNS (green filled circle). **B**) Conditional expression of Gal80, a repressor of Gal4 activity, in all cells using an Actin5C promoter, subject to excision by Cre (gray shading indicates repression of Gal4). **C**) Selective activation of Cre in specific NBs (red dotted circle) to excise Gal80 and permit expression of the marker tdTomato (red stripes) and activity of Gal4 (solid green) in neurons derived from those NBs. **D**) Use of split Cre components to target NBs at the intersection of two NB expression patterns (red and blued dotted circles) to permit Gal4 activity selectively within cells derived from these NBs (solid green).

(E) Primary sequence of the Cre protein using the single letter amino acid code. Residues that participate in DNA-binding (blue) or catalysis (yellow highlight) are indicated as are the break-points (green highlight) chosen to generate the split Cre fragments for fusion to split inteins: Cre_A, Cre_B, Cre_{AB}, and Cre_C as indicated (magenta boxes).

(F-G) The bipartite SpaRCLIn system. **F**) Schematics of the Cre fragments fused to NrdJ-1 split inteins, indicating their ability to reconstitute full-length Cre, **G**) Cre_{AB} expression is directed to all NBs (white plus red shading) using the NB-specific DNE enhancer (see text), and Cre_C expression is directed to a subset of NBs (red) by the NBE enhancer, which will also express in other cell types (gray). Only the NBs targeted by NBE will express both Cre_{AB} and Cre_C and reconstitute full-length Cre.

(H-I) The tripartite SpaRCLIn system. **H**) Similar to (F) except that the CreAB fragment has been further divided into Cre_A and Cre_B components which have been fused to gp41-1 split

inteins at breakpoints. All three fragments are now required to reconstitute full-length Cre. **I**) Venn diagram similar to (G) indicating the intersection of the three enhancers used to drive Cre_A (DNE), Cre_B (NBE_2), and Cre_C (NBE_1).

J) Schematic of the floxed Gal80 construct used in the SpaRCLIn system, the expression of which is driven by the ubiquitously active Actin5C promoter. Cre-mediated excision of Gal80 via the flanking loxP sites causes a myristoylated tdTomato (tdTom) red fluorescent protein to be expressed instead of Gal80.

(K-M) Restriction of NB expression by SpaRCLIn. **K, L**) tdTom expression (red) driven by the bipartite SpaRCLIn system using two different NBEs (44F03 and 43H02) to drive CreC expression. **M**) tdTom expression driven by the tripartite SpaRCLIn system at the intersection of the two NBE expression patterns, which overlap in several NB pairs of the ventral nerve cord (VNC) and brain (Br). Neuropil labeling by the nc82 antibody is shown in blue. Scale bar: 50μM.

Note that the genotypes of the flies for panels of this and all subsequent figures are provided in Supplementary Table 2.

Figure 1-figure supplement 1. Expression patterns of neuroblast-active enhancers

(A-I) Nine representative examples of CNS expression of the 134 neuroblast-active enhancers (NBEs) used in this study. Shown are volume-rendered confocal micrographs of larval CNS whole mounts taken from animals expressing tdTomato in NB lineages in which the indicated enhancers are active. The expression patterns were generated using the bipartite SpaRCLIn system described in Fig. 1 to drive the tdTomato reporter in the labeled neuroblast lineages. Some of the NBEs show limited expression, as in (**A**), where only a single major neuroblast lineage with multiple, clustered progeny is labeled (arrow). Most, however, express in multiple

NBs broadly distributed throughout the brain (Br) and ventral nerve cord (VNC), as in (**E**), where the arrows indicate some of the larger NB clones with many labeled progeny. The number of progeny in NB clones could be as small as one to two cells as in (**B;** arrows), indicating that NBEs could be active in some NBs only at later stages of neurogenesis where they would thus label sublineages. Scale bar: 50μM.

Figure 1—figure supplement 2. A neuroblast-specific *deadpan-nerfin-1* enhancer, DNE

(A) Sequence of the chimaeric neuroblast enhancer used in this study, which is composed of an enhancer for the gene encoding the transcriptional repressor, *deadpan* (blue) fused via a 10 bp linker (red) to an enhancer for the gene encoding *nerfin-1* (black). Upper case letters signify the highly conserved sequences used to identify the enhancers using the Evoprinter. Underlined are conserved sequence blocks shared by the two enhancers that represent putative transcription factor binding sites. Yellow highlight indicates two nucleotide substitutions that expand the range of the *nerfin-1* enhancer expression in NBs. For further details see Materials and Methods. **(B**) Cis-regulatory activity of the DNE. The DNE was used to drive Gal4 expression, which was monitored during embryonic development by mRNA *in situ* hybridization. Shown are filleted wholemount embryos, stages 8-13 (anterior up). Most, if not all, CNS NBs are labeled during early to late stages of lineage development. Scale bar: 50μM.

Figure 2. Parsing the TH-Gal4 expression pattern using SpaRCLIn

(A) Expression pattern of the TH-Gal4 driver revealed by UAS-mCD8GFP (green). In all panels: Anti-nc82 labeled neuropil (magenta); ventral nerve cord; VNC; brain; Br.

(B-D) Restriction of TH-Gal4 expression using SpaRCLIn. **B, C**) mCD8GFP expression (green) in mature dopaminergic neurons isolated using the bipartite SpaRCLIn system and two different

NBEs (R44F03 and R52B02) to drive Cre_C expression. A neuronal pair common to both patterns is indicated (yellow arrows). **D**) mCD8GFP expression (green) driven by the tripartite SpaRCLIn system at the intersection of the two NBE expression patterns in B and C.

(E-H) Examples of TH-Gal4 restriction to small numbers of neurons using the tripartite system and the indicated pairs of NBEs. Scale bar: 50μM.

I) Size and stereotypy of the restricted expression patterns produced by the indicated Step 2 intersections. The average number of neurons per preparation (± standard deviation) observed for each intersection is shown together with the number of preparations examined. For each, intersection the neuron that was most frequently observed across preparations (i.e. the "principal common neuron") was identified and the percentage of preparations containing this neuron is shown in the bar graph (black bars) together with the percentage of preparations showing expression only in other neurons (gray bars) or no expression (white bars). Examples of principal common neurons are indicated by yellow arrows in D-H.

Figure 2-figure supplement 1. Stochastic expression within the TH-Gal4 pattern generated by SpaRCLIn

(A-G) Seven distinct restrictions of the TH-Gal4 expression pattern produced by the same pair of NBEs: R44F09-Cre_B∩R52B02-Cre_C. For five of the CNS preparations (**A-E**), labeling of one or more neurons was observed only in the brain (Br), while in two preparations labeling was observed in cells of both the ventral nerve cord (VNC) and brain (**F**), or in the VNC alone (**G**). The identity of all neurons isolated in these preparations appeared to be unique. Anti-nc82 labeled neuropil (magenta); UAS-mCD8GFP (green). Scale bar: 50μM.

Figure 2-figure supplement 2. Reproducibility of SpaRCLIn labeling within the TH-Gal4 pattern generated by SpaRCLIn

Expression patterns of all 16 CNS preparations for TH-Gal4$^{R14E10\text{-}Cre_B \cap R10C04\text{-}Cre_C}$. Yellow labels (a-c) identify the somata of neurons identified to be the same in different preparations, based on position and morphology. The neuron labeled "a" represents the primary expression pattern in that it occurs with the greatest frequency (8/16 preparations). Neurons "b" and "c" recur in 5 and 6 of the 16 preparations, respectively. In some cases, both neurons of these bilateral pairs are labeled, while in others only a single neuron is labeled. In all panels: Anti-nc82 labeled neuropil (magenta); UAS-mCD8GFP (green). Scale bar: 50μM.

Figure 3. Identification of command neurons for PE within the rk^{pan}- Gal4 pattern

(**A**) Induced PE (arrowhead) in a fly expressing the heat-sensitive ion channel dTrpA1 under the control of the rk^{pan}-Gal4 driver. Labels as described in the legend of Fig. 2A.

(**B**) Expression pattern of the rk^{pan}-Gal4 driver revealed by UAS-mCD8GFP (green). In all panels: Anti-nc82 labeled neuropil (magenta); ventral nerve cord: VNC; brain: Br.

(**C-D**) mCD8GFP expression (green) in mature subsets of RK-expressing neurons isolated using the bipartite SpaRCLIn system and NBEs R44F09 and R516H11 to drive Cre$_C$ expression.

(**E**) PE induced in a fly expressing dTrpA1 in the PE^{rk} neurons, isolated using the tripartite system with the R44F09 and R16H11 NBEs to parse the rk^{pan}-Gal4 pattern.

(**F-H**) Typical expression patterns in rk^{pan}-Gal4$^{R44F09 \cap R16H11}$ flies, showing expression in both bilateral pairs of PE^{rk} neurons (**F**), one neuron of each of the two bilateral pairs of PE^{rk} neurons (**G**), or no neurons (**H**). All scale bars: 50μM.

Figure 3-figure supplement 1. Workflow for SpaRCLIn Screens

(**A**) Crossing scheme for implementing a Step 1 screen using the bipartite SpaRCLIn system. The example given illustrates the strategy to be used when the Gal4 driver is on chromosome III, but reagents for use when the driver is on chromosome II are also provided (see Key Resources Table). An initial set of crosses brings the Gal4 driver together with two essential components of SpaRCLIn: an X chromosome containing the combined Actin 5C-loxP-Gal80-loxP-tdTomato and UAS-mCD8GFP constructs (abbreviated here as Cre80Tom-GFP) and a 2nd chromosome containing the DNE-Cre$_{AB}$. If a functional screen is being performed, an effector—such as UAS-dTrpA1—can also be recombined with the DNE-Cre$_{AB}$ or Gal4 driver on an autosome, as illustrated here. Alternatively, we have made variants of the Cre80Tom-GFP (on X) that contain UAS-dTrpA1 (Cre80-dTrpA1) or Kir2.1 (Cre80-Kir2.1) that can be used instead of Cre80Tom-GFP. Flies bearing the Gal4 driver and essential SpaRCLIn components, are then crossed in a final step to flies of the Cre$_C$ library to generate the desired progeny for testing. The NBEs of those Cre$_C$ library lines that test positive (e.g. NBE$_n$-Cre$_C$ and NBE$_m$-Cre$_C$) can then be used for intersectional analysis in a Step 2 tripartite screen. This is done by combining one of the NBE-Cre$_C$ components, say NBE$_n$-Cre$_C$, with the NBE$_m$-Cre$_B$ component, which is readily accomplished by a series of genetic crosses (dotted arrow) because all NBE-Cre$_C$ inserts are on chromosome III, and all NBE-Cre$_B$ inserts are on II.

(**B**) Crossing scheme for a tripartite SpaRCLIn screen. Initial crosses similar to those described for the bipartite screen are performed to combine essential SpaRCLIn components together with the Gal4 driver. Now, however, DNE-Cre$_A$ is used instead of DNE-Cre$_{AB}$. Progeny with the final genotype for testing are generated using flies made as described in A that combine NBE-Cre$_B$ and -Cre$_C$ components.

Figure 3-figure supplement 2. Dicistronic vector with floxed Gal80 and UAS constructs

(**A**)rk^{pan}-Gal4 Schematic of the plasmid used to make flies with the Cre80Tom construct and either the UAS-mCD8GFP, UAS-dTrpA1, or UAS-Kir2.1 construct. The latter are inserted into the plasmid via a unique NdeI restriction site in the plasmid.

(**B**) Annotated sequence of the Cre80Tom-GFP expression construct.

Figure 3-figure supplement 3. rk$^{R16H11\text{-}Cre_B \cap R25G06\text{-}Cre_C}$-Gal4 expression patterns include PE^{rk} and other neurons.

(**A-C**) Three representative examples of the labeling patterns obtained with the R16H11-Cre_B∩R25G06-Cre_C enhancer pair in the tripartite SpaRCLIn system. All animals whose expression was restricted in this way (n=14) showed induced PE when expressing dTrpA1 and all had expression in the PE^{rk} neurons of the SEZ. In addition, however, each preparation also exhibited expression in a range of other neurons (arrows). Scale bar: 50μM.

Figure 4. Limiting Cre activity to early NBs using FRTerminator

(**A**) The FRTerminator construct: a DNE-Cre_{AB} that terminates its own expression. The FRTerminator expression cassette contains sequences for the Flp recombinase and Cre_{AB}-NrdJ-1^N linked by a viral T2A sequence to ensure separate translation of the two gene products. The entire cassette is flanked by FRT sites. Upon expression of the cassette—which will occur in NBs at the onset of neurogenesis—Flp will excise the cassette, thus terminating any further expression of both Flp and Cre_{AB}-NrdJ-1^N.

(**B**) Schematic comparing the consequences of DNE-Cre_{AB} (left box) and FRTerminator (right box) action in two NB lineages (NB_1 and NB_2) in which an NBE (used to drive expression of Cre_C) is active. In NB_1 the NBE is active early in neurogenesis and Cre_C will therefore be expressed in the young neuroblast. In contrast, the NBE becomes active only late in neurogenesis

in NB_2 and Cre_C is therefore only present in the older NB. Because DNE-Cre_{AB} is expressed throughout neurogenesis, it will be available to reconstitute full-length Cre whenever Cre_C is expressed. This means that Gal80 will be excised and tdTomato expression turned on (red) early in NB_1—leading to the labeling of all progeny—and late in NB_2—leading to labeling of only late-generated progeny. In contrast, FRTerminator is present only early in neurogenesis and Cre reconstitution (and tdTomato expression) will therefore occur only in NB_1. No progeny of the NB_2 clone will be labeled and the overall pattern of labeling will thus be diminished.

(C-D) NB lineages targeted using NBE_{R16H11}-Cre_C and either the DNE-Cre_{AB} construct of the bipartite SpaRCLIn system (**C**), or FRTerminator (**D**). NB progeny are visualized with tdTomato (red) after excision of Gal80 by Cre. The breadth of tdTomato expression when using DNE-Cre_{AB} compared with FRTerminator reflects the loss of sublineages generated by NBs in which the R16H11 enhancer becomes active only later in neurogenesis, as illustrated in B. Anti-nc82 labeled neuropil (blue); ventral nerve cord; VNC; brain; Br. Scale bar: 50µM.

(**E-F**) Restriction of the rk^{pan}-Gal4 expression pattern by SpaRCLIn using R14E10-Cre_C with DNE-Cre_{AB} (**E**) or FRTerminator (**F**). FRTerminator significantly reduces the expression pattern compared with the restriction obtained with DNE-Cre_{AB}, labeling principally the PE^{rk} neurons. Reporter: UAS-mCD8GFP (green); Anti-nc82 labeled neuropil (magenta); ventral nerve cord; VNC; brain; Br. Scale bar: 50µM.

Videos

Video 1. Activation of neurons in the rk^{pan}-Gal4 pattern induces robust proboscis extension.

rk^{pan}-Gal4 was used to drive expression of the heat-activated ion channel, UAS-dTrpA1. At 18°C the channel is inactive and animals expressing it throughout the rk^{pan}-Gal4 pattern do not extend their proboscis. In contrast, at 31°C when the channel is activated, animals display prolonged proboscis extension.

Video 2. Activation of the PE^{rk} neurons induces robust, rhythmic proboscis extension.

The tripartite SpaRCLIn system isolates a subset of neurons within the rk^{pan}-Gal4$^{DNE\text{-}Cre_A \cap R16H11\text{-}Cre_B \cap R44F09\text{-}Cre_C}$ intersection called the PE^{rk} neurons. When activated using dTrpA1 and a temperature of 31°C repeated, rhythmic proboscis extension is induced.

Video 3. Neuroanatomical location and projection pattern of the PE^{rk} neurons.

GFP-labeled PE^{rk} neurons (green) were imaged by confocal microscopy to show the location of their somata and their arborization. Neuropil labeled by nc82 antibody is shown in blue to identify brain regions.

References:

Asahina, K., Watanabe, K., Duistermars, B.J., Hoopfer, E., Gonzalez, C.R., Eyjolfsdottir, E.A., Perona, P., and Anderson, D.J. (2014). Tachykinin-Expressing Neurons Control Male-Specific Aggressive Arousal in Drosophila. Cell *156*, 221-235.

Aso, Y., Hattori, D., Yu, Y., Johnston, R.M., Iyer, N.A., Ngo, T.T.B., Dionne, H., Abbott, L.F., Axel, R., Tanimoto, H.*, et al.* (2014). The neuronal architecture of the mushroom body provides a logic for associative learning. Elife *3*.

Awasaki, T., Kao, C.F., Lee, Y.J., Yang, C.P., Huang, Y.L., Pfeiffer, B.D., Luan, H.J., Jing, X.T., Huang, Y.F., He, Y.S.*, et al.* (2014). Making Drosophila lineage-restricted drivers via patterned recombination in neuroblasts. Nat Neurosci *17*, 631-U203.

Bohm, R.A., Welch, W.P., Goodnight, L.K., Cox, L.W., Henry, L.G., Gunter, T.C., Bao, H., and Zhang, B. (2010). A genetic mosaic approach for neural circuit mapping in Drosophila. Proc Natl Acad Sci U S A *107*, 16378-16383.

Brody, T., Yavatkar, A.S., Kuzin, A., Kundu, M., Tyson, L.J., Ross, J., Lin, T.Y., Lee, C.H., Awasaki, T., Lee, T.*, et al.* (2012). Use of a Drosophila genome-wide conserved sequence database to identify functionally related cis-regulatory enhancers. Dev Dynam *241*, 169-189.

Brust, R.D., Corcoran, A.E., Richerson, G.B., Nattie, E., and Dymecki, S.M. (2014). Functional and Developmental Identification of a Molecular Subtype of Brain Serotonergic Neuron Specialized to Regulate Breathing Dynamics. Cell Rep *9*, 2152-2165.

Carvajal-Vallejos, P., Pallisse, R., Mootz, H.D., and Schmidt, S.R. (2012). Unprecedented Rates and Efficiencies Revealed for New Natural Split Inteins from Metagenomic Sources. J Biol Chem *287*, 28686-28696.

Diao, F.Q., and White, B.H. (2012). A Novel Approach for Directing Transgene Expression in Drosophila: T2A-Gal4 In-Frame Fusion. Genetics *190*, 1139-U1356.

Dionne, H., Hibbard, K.L., Cavallaro, A., Kao, J.C., and Rubin, G.M. (2018). Genetic Reagents for Making Split-GAL4 Lines in Drosophila. Genetics *209*, 31-35.

Doe, C.Q. (2017). Temporal Patterning in the Drosophila CNS. Annu Rev Cell Dev Bi *33*, 219-240.

Dolan, M.J., Luan, H.J., Shropshire, W.C., Sutcliffe, B., Cocanougher, B., Scott, R.L., Frechter, S., Zlatic, M., Jefferis, G.S.X.E., and White, B.H. (2017). Facilitating Neuron-Specific Genetic Manipulations in Drosophila melanogaster Using a Split GAL4 Repressor. Genetics *206*, 775-784.

Dymecki, S.M., Ray, R.S., and Kim, J.C. (2010). Mapping Cell Fate and Function Using Recombinase-Based Intersectional Strategies. Method Enzymol *477*, 183-213.

Emery, J.F., and Bier, E. (1995). Specificity of Cns and Pns Regulatory Subelements Comprising Pan-Neural Enhancers of the Deadpan and Scratch Genes Is Achieved by Repression. Development *121*, 3549-3560.

Flood, T.F., Iguchi, S., Gorczyca, M., White, B., Ito, K., and Yoshihara, M. (2013). A single pair of interneurons commands the Drosophila feeding motor program. Nature *499*, 83-+.

Friggi-Grelin, F., Coulom, H., Meller, M., Gomez, D., Hirsh, J., and Birman, S. (2003). Targeted gene expression in Drosophila dopaminergic cells using regulatory sequences from tyrosine hydroxylase. J Neurobiol *54*, 618-627.

Gao, Q., and Finkelstein, R. (1998). Targeting gene expression to the head: the Drosophila orthodenticle gene is a direct target of the Bicoid morphogen. Development *125*, 4185-4193.

Garcia-Marques, J., Yang, C.P., Espinosa-Medina, I., Mok, K., Koyama, M., and Lee, T. (2019). Unlimited Genetic Switches for Cell-Type-Specific Manipulation. Neuron.

Ge, J., Wang, L.J., Yang, C., Ran, L.Y., Wen, M.L., Fu, X.A., Fan, D., and Luo, K.M. (2016). Intein-mediated Cre protein assembly for transgene excision in hybrid progeny of transgenic Arabidopsis. Plant Cell Rep *35*, 2045-2053.

Gohl, D., Morante, J., and Venken, K. (2017). The Current State of the Neuroanatomy Toolkit in the Fruit Fly Drosophila melanogaster. In Decoding Neural Circuit Structure and Function: Cellular Dissection Using Genetic Model Organisms, A. Celik, and M. Wernet, eds. (Springer), pp. 3-40.

Gordon, M.D., and Scott, K. (2009). Motor control in a Drosophila taste circuit. Neuron *61*, 373-384.
Hampel, S., Chung, P., McKellar, C.E., Hall, D., Looger, L.L., and Simpson, J.H. (2011). Drosophila Brainbow: a recombinase-based fluorescence labeling technique to subdivide neural expression patterns. Nat Methods *8*, 253-259.

Han, X.Z., Han, F.Y., Ren, X.S., Si, J., Li, C.Q., and Song, H.Y. (2013). Ssp DnaE split-intein mediated split-Cre reconstitution in tobacco. Plant Cell Tiss Org *113*, 529-542.

Harris, R.M., Pfeiffer, B.D., Rubin, G.M., and Truman, J.W. (2015). Neuron hemilineages provide the functional ground plan for the Drosophila ventral nervous system. Elife *4*.

Heidmann, D., and Lehner, C.F. (2001). Reduction of Cre recombinase toxicity in proliferating Drosophila cells by estrogen-dependent activity regulation. Dev Genes Evol *211*, 458-465.

Hermann, M., Stillhard, P., Wildner, H., Seruggia, D., Kapp, V., Sanchez-Iranzo, H., Mercader, N., Montoliu, L., Zeilhofer, H.U., and Pelczar, P. (2014). Binary recombinase systems for high-resolution conditional mutagenesis. Nucleic Acids Res *42*, 3894-3907.

Hirrlinger, J., Scheller, A., Hirrlinger, P.G., Kellert, B., Tang, W.N., Wehr, M.C., Goebbels, S., Reichenbach, A., Sprengel, R., Rossner, M.J*., et al.* (2009). Split-Cre Complementation Indicates Coincident Activity of Different Genes In Vivo. Plos One *4*.

Hobert, O. (2016). Terminal Selectors of Neuronal Identity. Curr Top Dev Biol *116*, 455-+.

Hobert, O., Glenwinkel, L., and White, J. (2016). Revisiting Neuronal Cell Type Classification in Caenorhabditis elegans. Curr Biol *26*, R1197-R1203.

Hobert, O., and Kratsios, P. (2019). Neuronal identity control by terminal selectors in worms, flies, and chordates. Current Opinion in Neurobiology *56*, 97-105.

Huang, Z.J. (2014). Toward a Genetic Dissection of Cortical Circuits in the Mouse. Neuron *83*, 1284-1302.

Itskov, P.M., Moreira, J.M., Vinnik, E., Lopes, G., Safarik, S., Dickinson, M.H., and Ribeiro, C. (2014). Automated monitoring and quantitative analysis of feeding behaviour in Drosophila. Nat Commun *5*.

Jazayeri, M., and Afraz, A. (2017). Navigating the Neural Space in Search of the Neural Code. Neuron *93*, 1003-1014.

Jenett, A., Rubin, G.M., Ngo, T.T.B., Shepherd, D., Murphy, C., Dionne, H., Pfeiffer, B.D., Cavallaro, A., Hall, D., Jeter, J.*, et al.* (2012). A GAL4-Driver Line Resource for Drosophila Neurobiology. Cell Rep *2*, 991-1001.

Jullien, N., Sampieri, F., Enjalbert, A., and Herman, J.P. (2003). Regulation of Cre recombinase by ligand-induced complementation of inactive fragments. Nucleic Acids Res *31*.

Kain, P., and Dahanukar, A. (2015). Secondary Taste Neurons that Convey Sweet Taste and Starvation in the Drosophila Brain. Neuron *85*, 819-832.

Kasture, A.S., Hummel, T., Sucic, S., and Freissmuth, M. (2018). Big Lessons from Tiny Flies: Drosophila melanogaster as a Model to Explore Dysfunction of Dopaminergic and Serotonergic Neurotransmitter Systems. Int J Mol Sci *19*.

Kawano, F., Okazaki, R., Yazawa, M., and Sato, M. (2016). A photoactivatable Cre-loxP recombination system for optogenetic genome engineering. Nat Chem Biol *12*, 1059-+.

Kennedy, M.J., Hughes, R.M., Peteya, L.A., Schwartz, J.W., Ehlers, M.D., and Tucker, C.L. (2010). Rapid blue-light-mediated induction of protein interactions in living cells. Nat Methods *7*, 973-U948.

Kuzin, A., Kundu, M., Brody, T., and Odenwald, W.F. (2011). Functional analysis of conserved sequences within a temporally restricted neural precursor cell enhancer. Mech Develop *128*, 165-177.

Kuzin, A., Kundu, M., Ross, J., Koizumi, K., Brody, T., and Odenwald, W.F. (2012). The cis-regulatory dynamics of the Drosophila CNS determinant castor are controlled by multiple sub-pattern enhancers. Gene Expr Patterns *12*, 261-272.

Lacin, H., Chen, H.M., Long, X., Singer, R.H., Lee, T., and Truman, J.W. (2019). Neurotransmitter identity is acquired in a lineage-restricted manner in the Drosophila CNS. Elife *8*.

Lee, T., and Luo, L. (1999). Mosaic analysis with a repressible cell marker for studies of gene function in neuronal morphogenesis. Neuron *22*, 451-461.

Luan, H., Peabody, N.C., Vinson, C.R., and White, B.H. (2006). Refined spatial manipulation of neuronal function by combinatorial restriction of transgene expression. Neuron *52*, 425-436.

Luan, H.J., Diao, F.Q., Peabody, N.C., and White, B.H. (2012). Command and Compensation in a Neuromodulatory Decision Network. Journal of Neuroscience *32*, 880-889.

Luo, L.Q., Callaway, E.M., and Svoboda, K. (2018). Genetic Dissection of Neural Circuits: A Decade of Progress. Neuron *98*, 256-281.

Manning, L., Heckscher, E.S., Purice, M.D., Roberts, J., Bennett, A.L., Kroll, J.R., Pollard, J.L., Strader, M.E., Lupton, J.R., Dyukareva, A.V.*, et al.* (2012). A Resource for Manipulating Gene Expression and Analyzing cis-Regulatory Modules in the Drosophila CNS. Cell Rep *2*, 1002-1013.

Marella, S., Mann, K., and Scott, K. (2012). Dopaminergic Modulation of Sucrose Acceptance Behavior in Drosophila. Neuron *73*, 941-950.

Nern, A., Pfeiffer, B.D., Svoboda, K., and Rubin, G.M. (2011). Multiple new site-specific recombinases for use in manipulating animal genomes. P Natl Acad Sci USA *108*, 14198-14203.

Okaty, B.W., Freret, M.E., Rood, B.D., Brust, R.D., Hennessy, M.L., Debairos, D., Kim, J.C., Cook, M.N., and Dymecki, S.M. (2015). Multi-Scale Molecular Deconstruction of the Serotonin Neuron System. Neuron *88*, 774-791.

Peabody, N.C., Pohl, J.B., Diao, F., Vreede, A.P., Sandstrom, D.J., Wang, H., Zelensky, P.K., and White, B.H. (2009). Characterization of the decision network for wing expansion in Drosophila using targeted expression of the TRPM8 channel. J Neurosci *29*, 3343-3353.

Pfeiffer, B.D., Jenett, A., Hammonds, A.S., Ngo, T.T., Misra, S., Murphy, C., Scully, A., Carlson, J.W., Wan, K.H., Laverty, T.R.*, et al.* (2008). Tools for neuroanatomy and neurogenetics in Drosophila. Proc Natl Acad Sci U S A *105*, 9715-9720.

Pfeiffer, B.D., Ngo, T.T., Hibbard, K.L., Murphy, C., Jenett, A., Truman, J.W., and Rubin, G.M. (2010). Refinement of tools for targeted gene expression in Drosophila. Genetics *186*, 735-755.

Rajaee, M., and Ow, D.W. (2017). A new location to split Cre recombinase for protein fragment complementation. Plant Biotechnol J *15*, 1420-1428.

Ren, Q.Z., Awasaki, T., Huang, Y.F., Liu, Z.Y., and Lee, T. (2016). Cell Class-Lineage Analysis Reveals Sexually Dimorphic Lineage Compositions in the Drosophila Brain. Curr Biol *26*, 2583-2593.

Ren, Q.Z., Awasaki, T., Wang, Y.C., Huang, Y.F., and Lee, T. (2018). Lineage-guided Notch-dependent gliogenesis by Drosophila multi-potent progenitors. Development *145*.

Ren, Q.Z., Yang, C.P., Liu, Z.Y., Sugino, K., Mok, K., He, Y.S., Ito, M., Nern, A., Otsuna, H., and Lee, T. (2017). Stem Cell-Intrinsic, Seven-up-Triggered Temporal Factor Gradients Diversify Intermediate Neural Progenitors. Curr Biol *27*, 1303-1313.

Ross, J., Kuzin, A., Brody, T., and Odenwald, W.F. (2015). cis-regulatory analysis of the Drosophila pdm locus reveals a diversity of neural enhancers. Bmc Genomics *16*.

Schwarz, O., Bohra, A.A., Liu, X.Y., Reichert, H., VijayRaghavan, K., and Pielage, J. (2017). Motor control of Drosophila feeding behavior. Elife *6*.

Shah, N.H., and Muir, T.W. (2011). Split Inteins: Nature's Protein Ligases. Isr J Chem *51*, 854-861.

Shah, N.H., and Muir, T.W. (2014). Inteins: nature's gift to protein chemists. Chem Sci *5*, 446-461.

Shang, Y.H., Griffith, L.C., and Rosbash, M. (2008). Light-arousal and circadian photoreception circuits intersect at the large PDF cells of the Drosophila brain. P Natl Acad Sci USA *105*, 19587-19594.

Stevens, A.J., Sekar, G., Shah, N.H., Mostafavi, A.Z., Cowburn, D., and Muir, T.W. (2017). A promiscuous split intein with expanded protein engineering applications. P Natl Acad Sci USA *114*, 8538-8543.

Tastekin, I., and Louis, M. (2017). Manipulation of Neural Circuits in Drosophila Larvae. In Decoding Neural Circuit Structure and Function: Cellular Dissection Using Genetic Model Organisms, A. Çelik, and M.F. Wernet, eds. (Cham, Switzerland: Springer), pp. 171-190.

Tirian, L.M., Fellner, M., and Dickson, B.J. (2017). The VT GAL4, LexA, and split-Gal4 collectino for targeted expression in the Drosophila nervous system. bioRxiv.

Wang, H., Liu, J., Yuet, K.P., Hill, A.J., and Sternberg, P.W. (2018). Split cGAL, an intersectional strategy using a split intein for refined spatiotemporal transgene control in &ITCaenorhabditis&IT &ITelegans&IT. P Natl Acad Sci USA *115*, 3900-3905.

Wang, P., Chen, T.R., Sakurai, K., Han, B.X., He, Z.G., Feng, G.P., and Wang, F. (2012). Intersectional Cre Driver Lines Generated Using Split-Intein Mediated Split-Cre Reconstitution. Sci Rep-Uk *2*.

Wang, Y.C., Yang, J.S., Johnston, R., Ren, Q.Z., Lee, Y.J., Luan, H.J., Brody, T., Odenwald, W.F., and Lee, T. (2014). Drosophila intermediate neural progenitors produce lineage-dependent related series of diverse neurons. Development *141*, 253-258.

Xie, T.T., Ho, M.C.W., Liu, Q.L., Horiuchi, W., Lin, C.C., Task, D., Luan, H.J., White, B.H., Potter, C.J., and Wu, M.N. (2018). A Genetic Toolkit for Dissecting Dopamine Circuit Function in Drosophila. Cell Rep *23*, 652-665.

Yavatkar, A.S., Lin, Y., Ross, J., Fann, Y., Brody, T., and Odenwald, W.F. (2008). Rapid detection and curation of conserved DNA via enhanced-BLAT and EvoPrinterHD analysis. Bmc Genomics *9*.

Zeng, H.K., and Sanes, J.R. (2017). Neuronal cell-type classification: challenges, opportunities and the path forward. Nat Rev Neurosci *18*, 530-546.

Materials and Methods:

Drosophila Stocks.

Vinegar flies of the species *Drosophila* melanogaster were used in this study. Unless otherwise noted, all flies were grown on BDSC Cornmeal Food and maintained at 25°C in a constant 12 h light–dark cycle. Both male and female progeny of the genotypes indicated in Supplementary Table 2 were used in this study. Previously described fly stocks and their sources are listed in the Key Resources Table. Fly lines generated for this study were made using the DNA constructs described below. Injection of these constructs to produce transgenic flies was carried out by Rainbow Transgenic Flies, Inc. (Camarillo, CA). All transgene insertions except the insertion of the DNE-Gal4 were mediated by ΦC31 integrase and placed in the defined attP landing sites indicated in Key Resources Table. Flies made with the DNE-Gal4 were generated by p-element mediated transgenesis. All other transgenic flies of the NBE-Cre_B library have transgene insertions on the 2nd chromosome at attP40, while all flies in the NBE-Cre_C library have insertions on the 3rd chromosome at either VK00033 or VK00027.

Molecular Biology.

All oligonucleotide and gBlock synthesis was carried out by Integrated DNA Technologies, Inc. (Coralville, Iowa), and all final constructs were verified by sequencing (Eurofins Scientific, Louisville, KY or Macrogen Corp, Rockville MD). For routine molecular biology, the following reagents were used according to the manufacturers' supplied protocols: PCR amplification: Q5 High-Fidelity 2X Master Mix #M0492S (New England Biolabs, Ipswich, MA); DNA ligation: Quick Ligation Kit #M2200L (New England Biolabs, Ipswich, MA); Cloning: Gateway LR Clonase II Enzyme mix #11791100 (Thermofisher Scientific, Waltham, MA), and In-Fusion HD Cloning Plus #638911(Takara Bio USA, Inc., Mountain View, CA).

gBlocks were used to generate most of the final and intermediate constructs described below, including the DNA fragments encoding the NrdJ-1 and gp41-1 split inteins and the Cre fragments described in the manuscript. DNA sequences of the split inteins were back-translated from the published protein sequences (Carvajal-Vallejos et al., 2012) and all sequences were codon biased for *Drosophila*. Sequences of all gBlock fragments and PCR primers are listed in Supplementary Table 3 The following reagents, which were used to make several constructs as indicated below, are all described in Pfeiffer et al. (2010): pBPGal80Uw-5, pBPLexA::P65, 10XUAS-IVS-myr::tdTomato, 10XUAS-mCD8::GFP, and pBPGAL80Uw-6.

Cre80Tom constructs

The indicated Cre80Tom constructs were made stepwise using the described procedures. *Cre80Tom*: Step 1 - Made the intermediate construct "M1:" an NgoMIV-gBlock013-AatII fragment, an AatII-Gal80-SV40-MfeI fragment (from pBPGal80Uw-5), and an MfeI-gBlock014-KpnI fragment were placed between the NgoMIV and KpnI restriction sites of pBPLexA::P65. Step 2: PCR amplified a KpnI-IVS-StuI-AgeI-myr-tdTomato fragment (Primer71 + Primer72, 10XUAS-IVS-myr::tdTomato as template) and a p10-XbaI fragment (Primer71a + Primer72a, using as template CCAP-IVS-Syn21-KZip^{+}-p10; (Dolan et al., 2017)) and used these to replace the KpnI-XbaI fragment of M1 using In-Fusion HD cloning to make the intermediate construct "M2." Gateway cloning of M2 was then performed to add the Actin5C promoter (Harris et al., 2015) and get the final Cre80Tom construct.

Cre80Tom-GFP: Step 1: A 10XUAS-mCD8GFP PCR fragment (template 10XUAS-mCD8::GFP, Primer59+Primer58) was inserted into the unique NdeI site between the mini-white gene and the attB sequence of the M1 vector. Step 2: A KpnI-IVS-Syn21-myr-

tdTomato-StuI PCR fragment (Primer75, Primer76, template:10XUAS-IVS-myr::tdTomato) and a StuI-p10-SpeI PCR fragment (primer HJ077, HJ078) were placed between the KpnI and SpeI restriction sites to replace the LexA::P65 fragment and to produce the intermediate construct "M3" using the In-Fusion HD cloning kit. Step 3: Used Gateway Cloning to add the Actin 5C promoter to produce the *Cre80Tom-GFP*.

Cre80-dTrpA1 and Cre80-Kir2.1: The sequence between the KpnI and NsiI of M3 (including the IVS-Syn21-myr-tdTomato-p10- and a small part of the mini-white gene) were replaced with gBlock25 by HD-infusion cloning to make the intermediate construct "M4." This step removed the tdTomato gene. The BglII-mCD8GFP-XbaI fragment of M4 were replaced with BglII-dTrpA1-XbaI (template: UAS-dTrpA1, gift from Paul Garrity) and BglII-EFGP-Kir2.1-XbaI (template UAS-EGFP-Kir2.1, gift of Sean Sweeney) PCR fragments and then the actin5C promoter was inserted by Gateway cloning to get *Cre80-dTrpA1* and *Cre80-Kir2.1*.

Split Cre constructs

All split Cre constructs were made by Gateway cloning (LR reaction). Two sets of destination vectors with split Cre components were made: one for use with entry clones containing promoters, and another for entry clones containing enhancers. The 134 NBE entry clones were combined with the latter to make the expression clones used to generate the Cre_B and Cre_C libraries.

To make the Cre_A (HJP-176) destination vectors for use with promoter entry clones, a KpnI-IVS-NheI fragment made from annealed oligonucleotides, a NheI-gBlock012-AgeI gBlocks fragment and an AgeI-PmeI-WPRE-HindIII PCR fragment (amplified from pBPGAL80Uw-6 using PrimerS472 and PrimerS473) were placed between the NheI and HindIII restriction sites of the pBPGw vector (Addgene Plasmid #17574 Pfeiffer et al., 2008). Other split Cre

destination vectors (i.e. HJP177~HJP180; see the Key Resources Table) were made by replacing the NheI-Cre_A-gp41-1^N-AgeI fragment in Cre_A (HJP-176) with fragments consisting of: NheI-gBlock010-SphI + SphI-gBlock011-AgeI (HJP177), NheI-gBlock008-BsaI+BsaI-gBlock009-AgeI (HJP178), NheI-gBlock007-AgeI (HJP179), or NheI-gBlock010-SphI+SphI-gBlock015-AgeI (HJP180). To create a set of destination vectors for use with enhancer entry clones ("the U-series"), an FseI-DSCP-KpnI synthetic core promoter (Pfeiffer et al., 2008) was made from annealed oligos and inserted between the FseI and KpnI restriction sites of each of the destination vectors made for use with promoter entry clones. This produced constructs HJP194~196, HJP-207 and HJP-208 (See Key Resources Table).

Prior to the production of transgenic fly lines, the functionality of all Cre constructs was validated in cultured S2 cells by placing the constructs under the control of the Actin5C promoter and testing in appropriate combinations for expression and activity using a floxed reporter construct.

DNE and NBE entry clones

DNE: A 2 kb region upstream of the *deadpan* gene previously shown to harbor a NB enhancer by Emery and Bier (Emery and Bier, 1995) was Evoprinted (Yavatkar et al., 2008) using the sequences of five *Drosophila* species (*D. sechellia*, *D. simulans*, *D. erecta*, *D. yakuba*, and *D. ananasseae*) in addition to *D. melanogaster*. A 607 bp region starting 899 nucleotides 5' of the transcription start exhibited highly conserved sequence blocks containing transcription factor binding sites, including three CAGCTG E-boxes commonly found in other NB enhancers (Brody et al., 2012). A PCR fragment containing this 607 bp region was cloned into the Bullfinch Gal4 reporter vector (Brody et al., 2012), and the DNE enhancer was made by inserting next to it a previously described mutant *nerfin-1* enhancer with two adjacent bp

substitutions (G→C and T→C) that were shown to expand the pattern of NB expression (Kuzin et al., 2011). The mutant nerfin-1 enhancer was amplified by PCR from pCRII-TOPO (Thermofisher Scientific, Waltham, MA) and is separated from the *dpn* enhancer by 10 bp of DNA sequence from the pCRII-TOPO vector, including the EcoRI site that was used to insert this enhancer adjacent to the *dpn* enhancer. A DNE vector for use in Gateway cloning was made by transferring the DNE enhancer into the pENTR-D-TOPO entry clone as a PCR fragment (primers: DNE-Sense and DNE-Antisense) using the pENTR™/D-TOPO™ Cloning Kit).

Most of the neuroblast-active enhancers used to make the NBE entry clones were from the JFRC Flylight Collection (Pfeiffer et al., 2008).Candidate Flylight enhancers were selected based either on their previous identification as embryonic neuroblast enhancers (active in subset of neuroblasts) (Manning et al., 2012) or on the presence of expression in NBs in the 3rd instar CNS as determined by visual inspection of the expression patterns at the Flylight website (https://www.janelia.org/project-team/flylight). To verify NB expression of the latter NBEs, Flylight Gal4 lines made with the candidate enhancers were pre-screened by crossing them to flies containing the CreStop (HJP225) and UAS-Cre_C (HJP266) constructs described below with the following genotype: w, DNE-Cre_B(attP8); UAS-Cre_C(attP40); CreStop (i.e. actin^STOP^tomato(attP2)), DNE-Cre_A(VK00027). CNS preparations of the progeny (third instar larvae or adults) were examined for tdTomato expression in NB clones. Selected JFRC Neuroblast active enhancers (NBEs) with “sparse” expression in neuroblasts were amplified by PCR or synthesized when PCR failed (Epoch Life Science, Inc., Missouri City, TX) and cloned into either the pCR8-GW-TOPO or pENTR-D-TOPO donor vectors. Primers listed at

the Flylight website were used to amplify most JFRC NBEs using genomic DNA from either y; cn bw sp [gift from James A. Kennison] or Canton S wildtype flies as template.

The cas-8 and CG7229-5 enhancers (Brody et al., 2012; Kuzin et al., 2012) were synthesized as gBlock fragments and cloned by HD-Infusion cloning. The pdm-2-37a (Ross et al., 2015), cas-5 (Kuzin et al., 2012), danR-1, svp-29, and tll-15 enhancer sequences (gifts from Jermaine Ross) were amplified as PCR fragments from plasmids and placed between the NotI and AscI sites of pENTR/D-TOPO vector. The entry clones for the *stg-14* (Wang et al., 2014) and *otd* (Asahina et al., 2014; Gao and Finkelstein, 1998) enhancers have been previously described.

FRTerminator

This construct (HJP-473) was made as follows: an AvrII and PmeI flanked DNA fragment (including partial nerfin-1 enhancer, FRT and Syn21-flipase-T2A-Cre_A-gp41-1^N-AgeI-FRT) were synthesized (Epoch Life Science, Inc., Missouri City, TX) and put between the AvrII and PmeI restriction sites of DNE-CreA-gp41-1^N.The resulting construct can be used in place of DNE-Cre_A in Step 2 SpaRCLIn screens. It was tested, but its use is not described in this manuscript. This construct was used as an intermediary to make the final FRTerminator construct by inserting gBlock-043 (part of the CreAB sequence and Nrdj-1N) into its SbfI and AgeI restriction sites using the In-Fusion HD cloning technique.

Other constructs

Two constructs were used to pre-screen candidate enhancers driving Gal4 expression. These included CreStop (HJP225) and UAS-Cre_C (HJP266). The CreStop construct was made using a NgoMIV-loxP-hsp70 terminator-MluI gBlock to replace the loxP-Gal80 in Cre80Tom (HJP223) by In-Fusion HD cloning. UAS-Cre_C was made by cloning a NotI-NrdJ-1^C-Cre_C-

XbaI PCR fragment (Primer116 and Primer117; Cre_C as template) between the NotI and XbaI sites of pJFRC1-10XUAS-mCD8::GFP using the In-Fusion HD cloning technique.

Immunostaining and Image Acquisition.

Excised nervous system whole mounts were prepared from wandering third-instar larvae or adults after dissection into PBS and fixation in 4% paraformaldehyde in PBS for 20–30 min. Immunostaining was done with the antibodies listed in the Key Resources Table at the indicated dilutions. For confocal imaging, all tissues were attached to poly-L-lysine coated cover glass and mounted in Vectashield (Vector Laboratories, Burlingame, CA) prior to imaging with a Nikon C-2 confocal microscope. Z-series were acquired in 0.85 µm increments using a 20× objective using 488 nm, 543 nm or 633nm laser emission lines for fluorophore excitation. The images shown are maximal projections of volume rendered z-stacks of confocal sections taken through the entire nervous system. NB expression of Gal4 driven by the DNE enhancer was examined in embryonic fillets by in situ hybridizations as previously described (Ross et al., 2015).

Proboscis extension assay.

Flies assayed for proboscis extension were raised at 25°C until the white prepupa stage and then transferred to 18°C until the time of testing. For neuronal activation using dTrpA1, the chambers were placed on the surface of the Echotherm Chilling/Heating Dry Bath IC25 (Torrey Pines Scientific, Inc., Carlsbad, CA) at 31°C. For the Step 1 SpaRCLIn screen, approximately a dozen adult flies (3-10 d old) of each genotype were placed in glass TriKinetics tubes (3 mm inner diameter; TriKinetics Inc, Waltham, MA) and videorecorded at 31°C for 3 minutes using a Sony NEX-VG10 videocamera. Proboscis extension behavior was analyzed from these recordings. If two or more flies exhibited robust, full-length extension,

the cross was scored as positive. For the Step 2 tripartite SpaRCLIn screen, two flies at a time (one male and one female) were videorecorded together in glass minichambers (0.3 cm diameter X 0.7 cm length) for 3 min at 18°C followed by 3 min at 31°C. Flies were subjected to these temperature transitions twice and proboscis extension behavior was analyzed following the recording. The criteria for positive proboscis extension was three or more bouts of full proboscis extension in both tests. For the FRTerminator behavior experiments flies were subjected to only one test. Flies used to make the videos included in the manuscript were back-mounted on a 200 uL pipette tip with 5-Minute-Rapid-Curing, General Purpose Adhesive Epoxy (ITW polymers Adhesive, Danvers, MA) and placed just above the heating plate, which was adjusted to apply temperature changes.

Figure 1

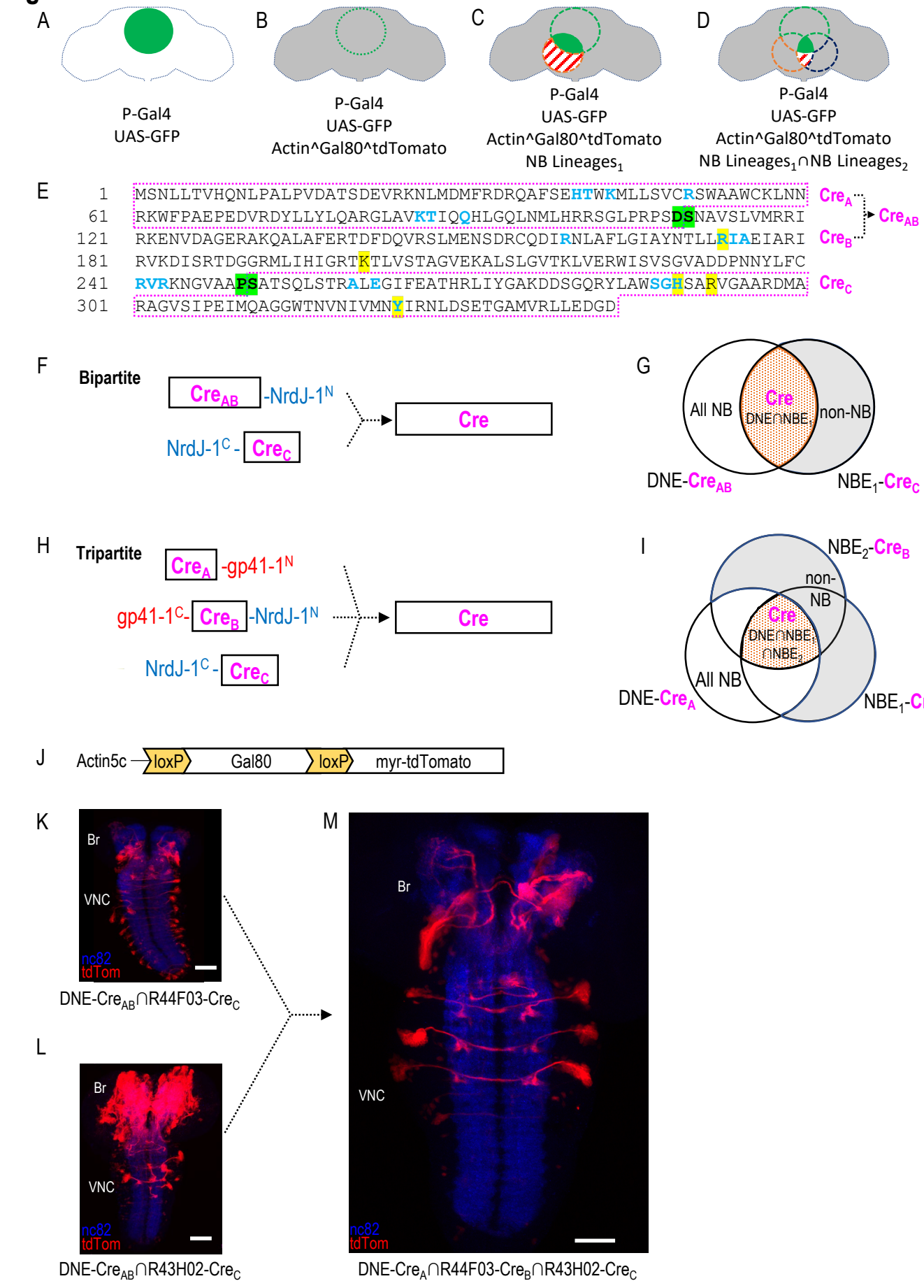
A
P-Gal4
UAS-GFP
B
P-Gal4
UAS-GFP
Actin^Gal80^tdTomato
C
P-Gal4
UAS-GFP
Actin^Gal80^tdTomato
NB Lineages1
D
P-Gal4
UAS-GFP
Actin^Gal80^tdTomato
NB Lineages1∩NB Lineages2
E
1 MSNLLTVHQNLPALPVDATSDEVRKNLMDMFRDRQAFSEHTWKMLLSVCRSWAAWCKLNN
61 RKWFPAEPEDVRDYLLYLQARGLAVKTIQQHLGQLNMLHRRSGLPRPSDSNAVSLVMRRI
121 RKENVDAGERAKQALAFERTDFDQVRSLMENSDRCQDIRNLAFLGIAYNTLLRIAEIARI
181 RVKDISRTDGGRMLIHIGRTKTLVSTAGVEKALSLGVTKLVERWISVSGVADDPNNYLFC
241 RVRKNGVAAPSATSQLSTRALEGIFEATHRLIYGAKDDSGQRYLAWSGHSARVGAARDMA
301 RAGVSIPEIMQAGGWTNVNIVMNYIRNLDSETGAMVRLLEDGD
CreA
CreB
CreC
CreAB
F
Bipartite
CreAB -NrdJ-1N
NrdJ-1C - CreC
Cre
G
All NB
Cre
DNE∩NBE1
non-NB
DNE-CreAB
NBE1-CreC
H
Tripartite
CreA -gp41-1N
gp41-1C- CreB -NrdJ-1N
NrdJ-1C - CreC
Cre
I
NBE2-CreB
non-NB
Cre
DNE∩NBE1 ∩NBE2
All NB
DNE-CreA
NBE1-CreC
J
Actin5c
loxP
Gal80
loxP
myr-tdTomato
K
Br
VNC
nc82
tdTom
DNE-CreAB∩R44F03-CreC
L
Br
VNC
nc82
tdTom
DNE-CreAB∩R43H02-CreC
M
Br
VNC
nc82
tdTom
DNE-CreA∩R44F03-CreB∩R43H02-CreC

Figure 1—figure supplement 1

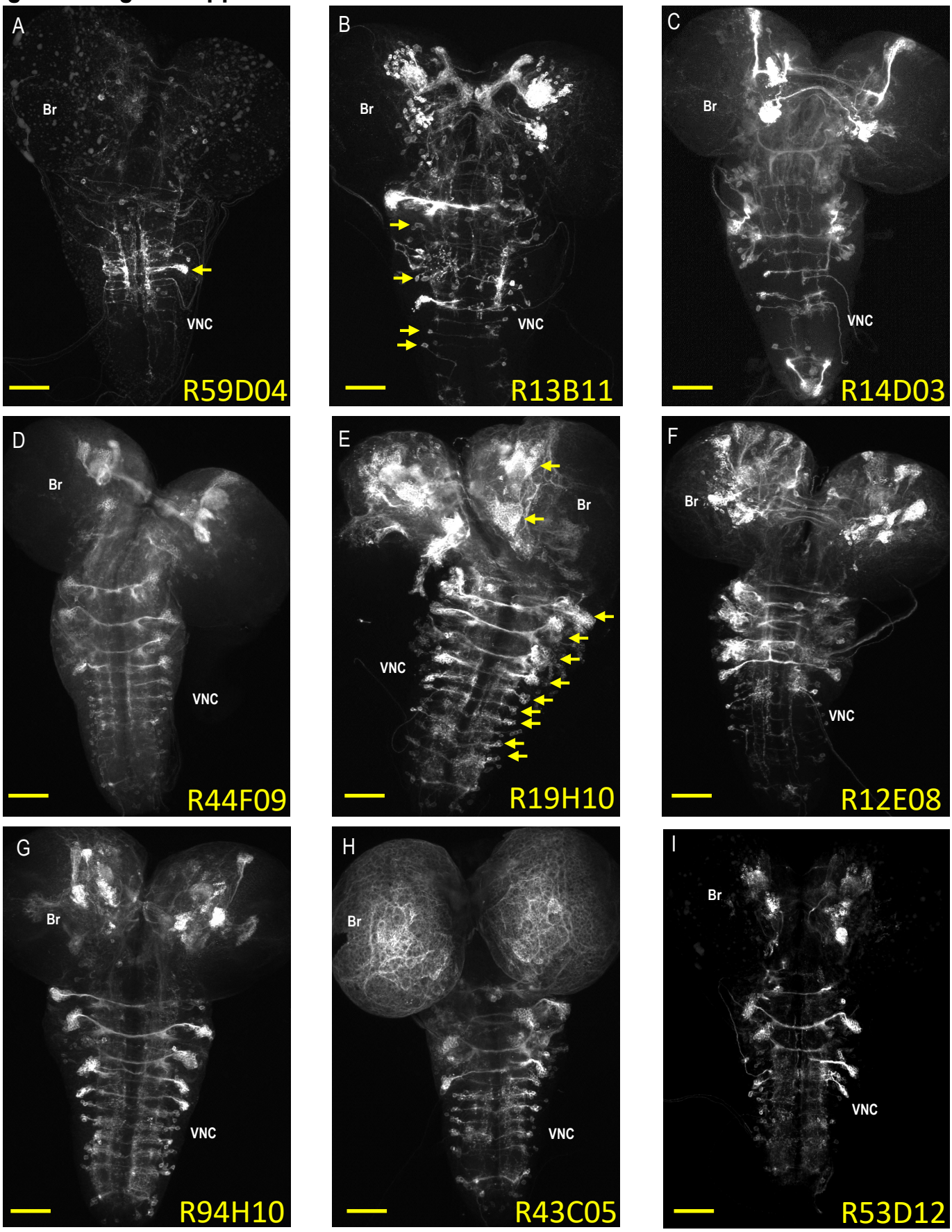

Figure 1—figure supplement 2

A

tcacTTTGCAcAACCAGgGTTGCCAGGCGGCGCAAtaCgTTTACgATCCCaCCcaaAAcTCCCCaaATCGgtccaTAG
GTAGATCTacGtCAGCTGTCAGCTGGCGCAtGgCCCGCGtCagTGGTTATTGACAACTCCTtTgGtCgTAATCCTGCC
AACATCGTAAAGTAATAAATTTGCCTGAAaAaGgAAAATcTGccGGgGATCGaCtATAAAAattGGCccAGcCAGGTA
AGCTcCGTAATGATTGACCCCGAccctcagtcccagacccacgaccgatccaggtccgattccgatccattgcaagtc
gcgattccgtcccgaaacccAAGCAACCCCCTTAAGACGcttctgccgatgagccggcCAGGCAAaAgcgaagaattt
gaaACTAAggatttcgccttgcAAGGGGGTTGGGtTGtCACgGGGGTTGCGGCAGCTGCGccgAACAATTGCCAAGGA
gtTCTCCTTAATGAATTGCAAATCATTCGccGGGCATTGATCAAGTTTGtCCttgCCAAGGGTGAaatctgtgcgact
aaatgtgccatcagccagccacccaaaagggaaacggacacaaacggaacatctgtcgcaagaattcgcccttgtgtc
tgctagtctgttaGTCTGtTACCTACCCCACCAAAAGCgAACTTGACgAGCTTAGTCGTCTGAGGCTGATAAATGCAG
TGCcgcaaagTACACctcgcgaaatttgtgtatgagatgtatgaaaaatgtaaaaatagatagcaatccgaactatgc
tccatgctaatgttcttcccagccgttaTTACtTGTTacaTTGTTTActTTTatAAcCAtcTTggccAACAGCTGTTT
aGcacCAAATGcCAAcaaAGAAaCAATTCACCTTttggcccAAGGATattCCCgatcTAttgatgaACCTtATGccTA
CatGCTCAATTAACGacTcCATGGgTGTCAGCTGTTTTTGGCAAAAAtaaGGACAATGTactGCTCaGATTTCCGCtG
AAtacacaaacatacatacatatttgcctagGAAGGTGCTGcGaTTTTGGTGCGTGGCAAttttgggtaccgaaacaa
CAGCTGTCgcacattGATTTctCCGAGTGCATTGTCCTggccgcaaaacgggagacTGTGTGTGTGTGTGcgtAGGAC
TTTCACTCCGtg

B

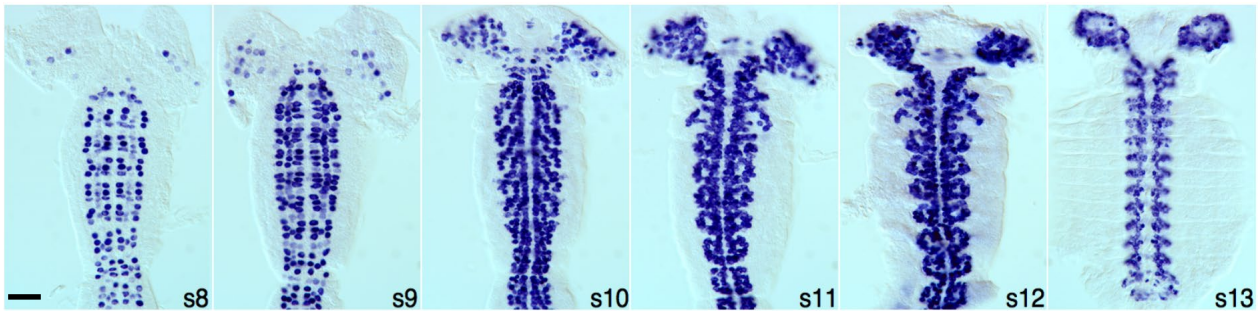

Figure 2

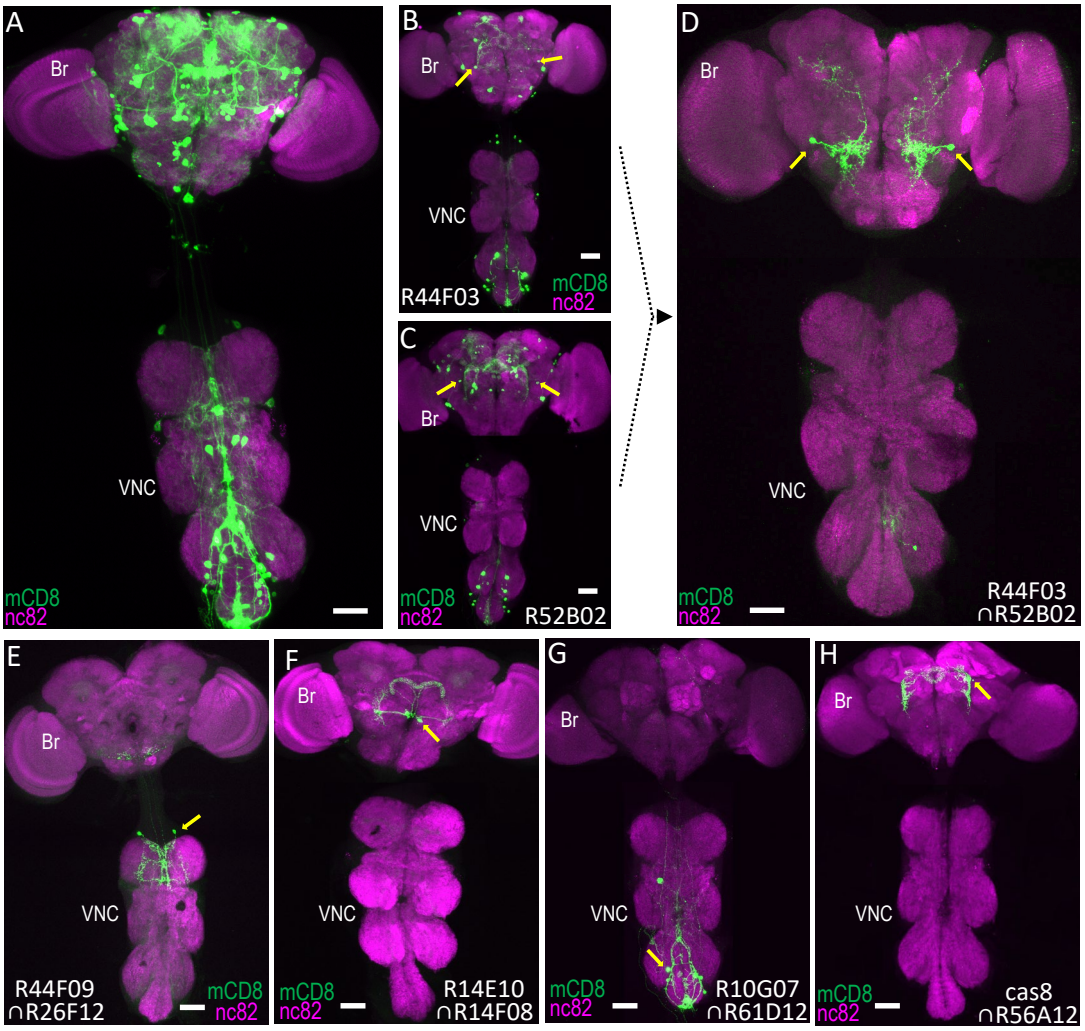

I

Intersection	Ave Cell #	n
R44F03∩R52B02	5.6 ± 2.0	15
R10G07∩R61D12	3.3 ± 1.9	18
R44F09∩R57B09	2.6 ± 1.3	16
R44F03∩R14F08	6.7 ± 4.4	13
R44F09∩R26F12	1.9 ± 0.8	12
R17A10∩R17A10	8.5 ± 3.8	16
R14E10∩R75A01	2.9 ± 1.1	12
R14E10∩R10C04	3.8 ± 2.0	16
R14E10∩R14F08	4.3 ± 2.3	17
R14E10∩R30A10	2.0 ± 0.9	10
cas-8∩R56A12	5.7 ± 3.0	18
R14E10∩R61D12	1.2 ± 0.5	9
R14E10∩R26F12	3.8 ± 1.8	9
R44F09∩ R52B02	1.9 ± 1.1	14

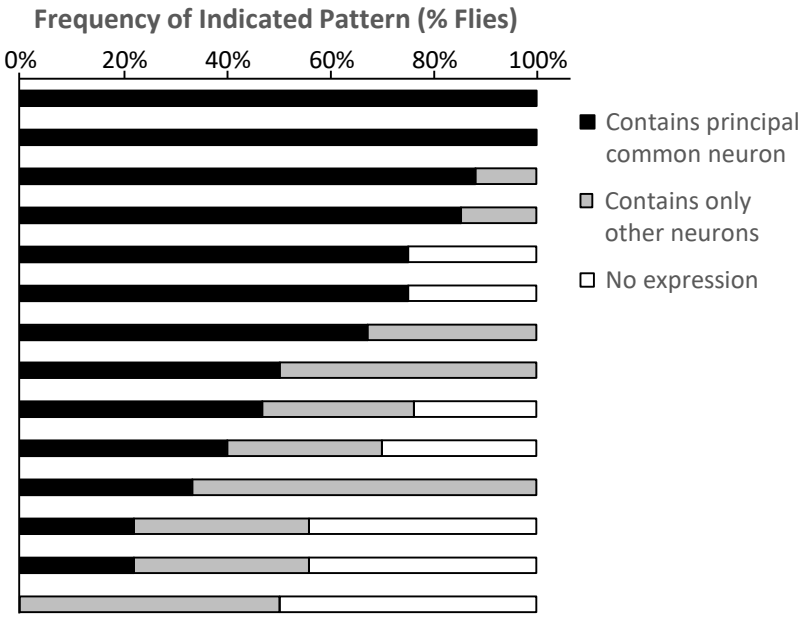

Figure 2—figure supplement 1

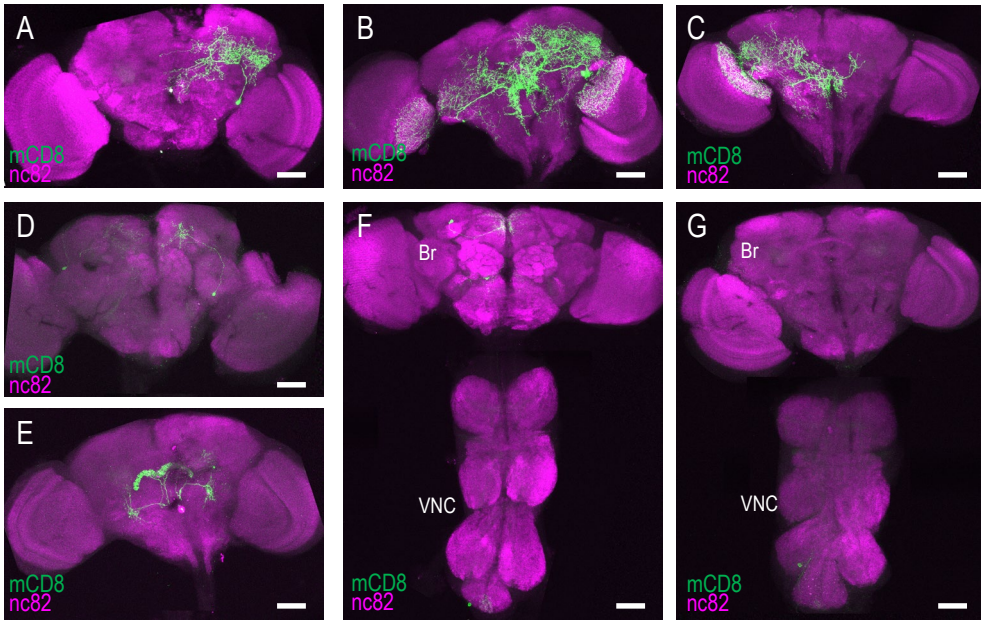

$TH\text{-}Gal4^{R44F09\text{-}Cre_B \cap R52B02\text{-}Cre_C}$

Figure 2—figure supplement 2

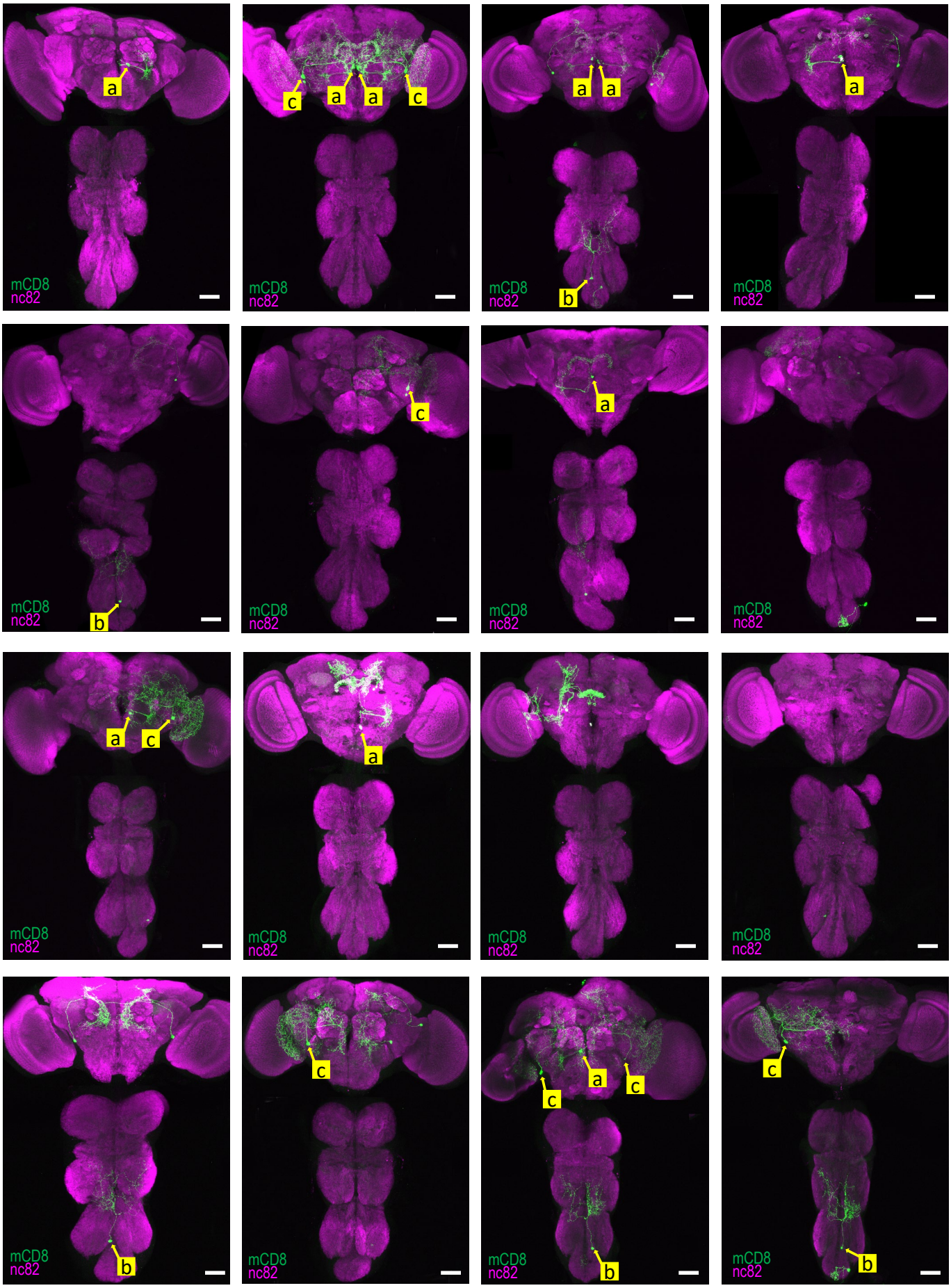

Figure 3

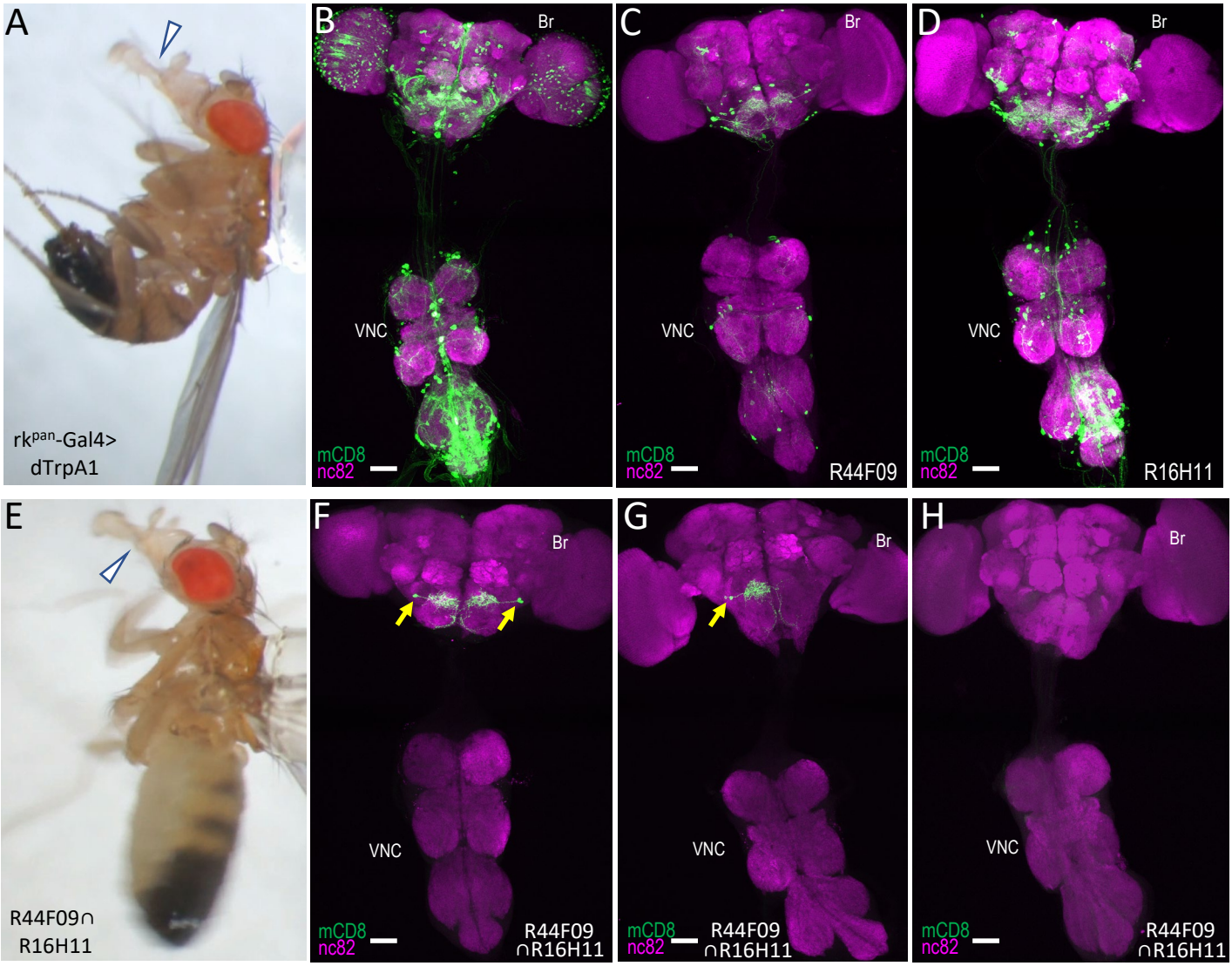
A
rk^pan-Gal4>
dTrpA1
B
Br
VNC
mCD8
nc82
C
Br
VNC
mCD8
nc82
R44F09
D
Br
VNC
mCD8
nc82
R16H11
E
R44F09∩
R16H11
F
Br
VNC
mCD8
nc82
R44F09
∩R16H11
G
Br
VNC
mCD8
nc82
R44F09
∩R16H11
H
Br
VNC
mCD8
nc82
R44F09
∩R16H11

Figure 3—figure supplement 1

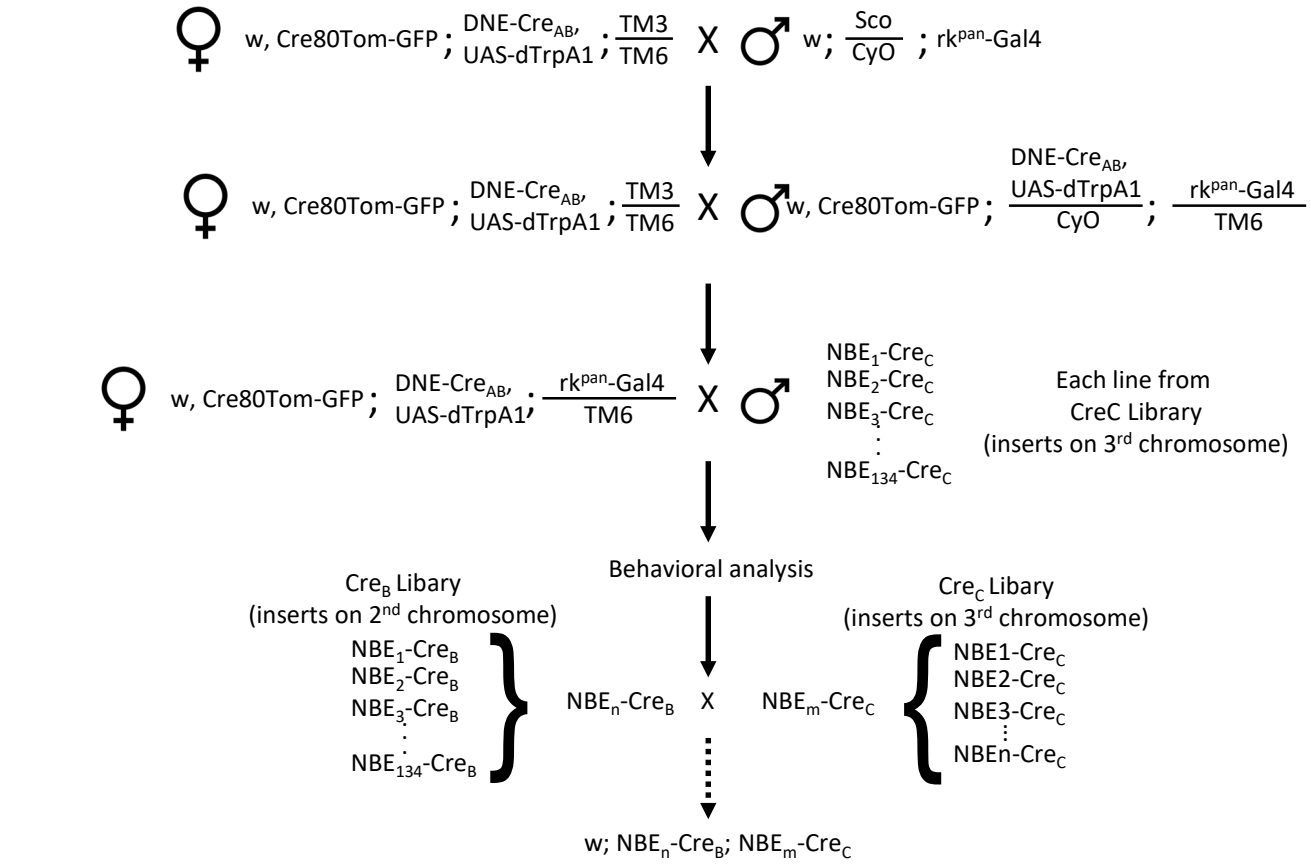

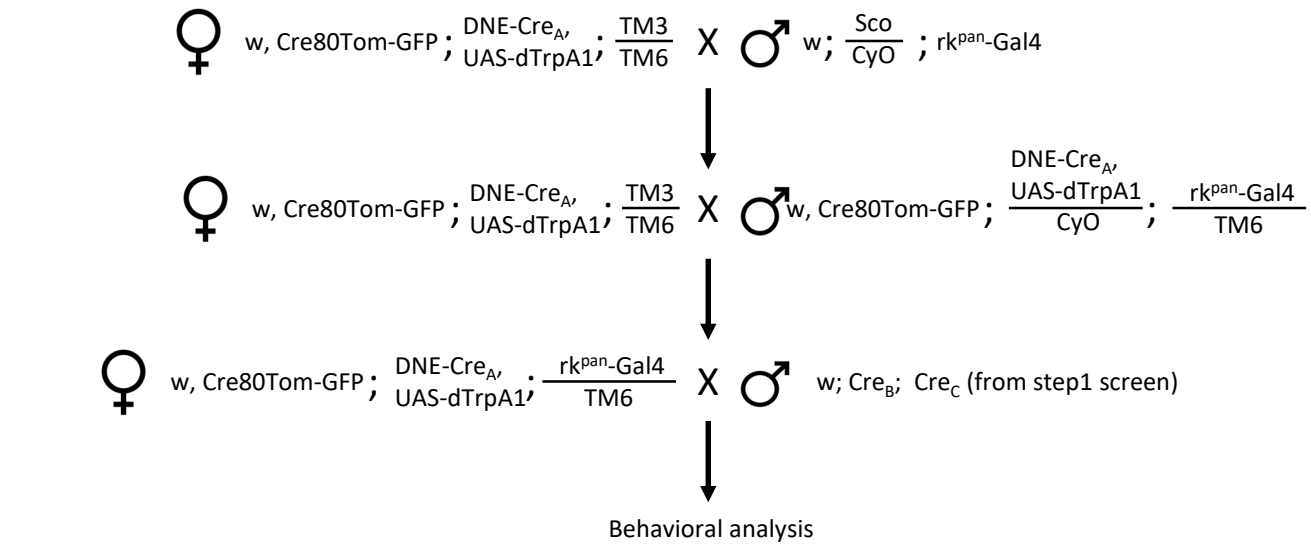

Figure 3—figure supplement 2

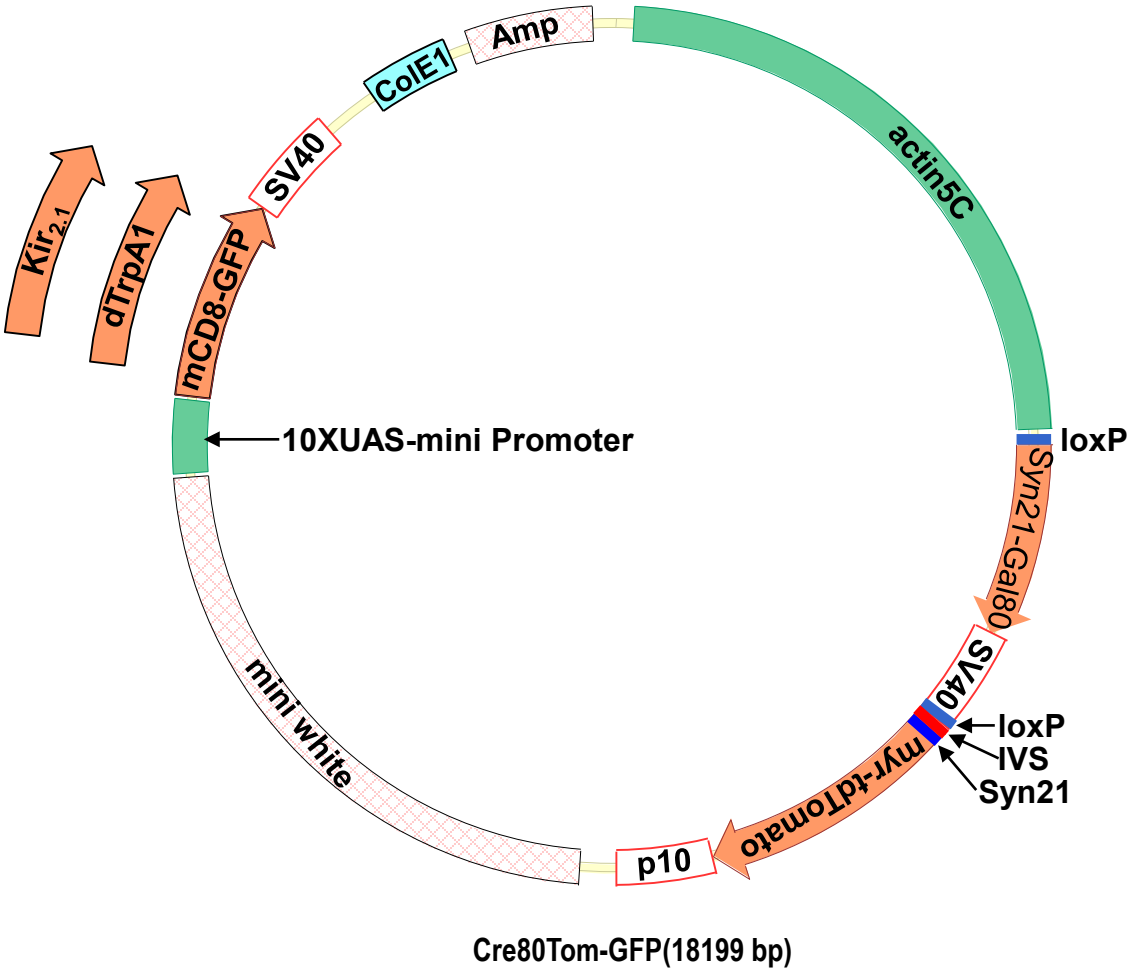

Cre80Tom-GFP(18199 bp)

Figure 3—figure supplement 3

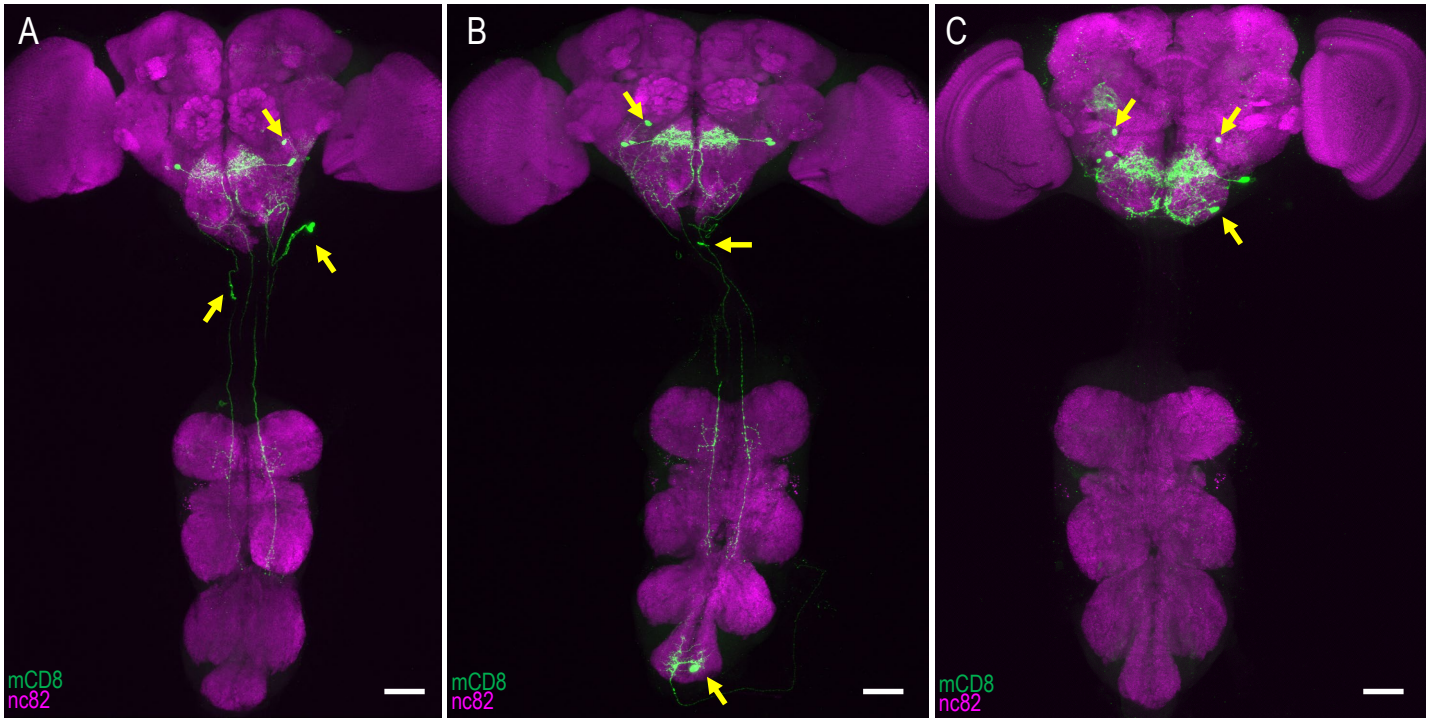

rk^{pan}-$Gal4^{R16H11\text{-}Cre_B \cap R25G06\text{-}Cre_C}$

Figure 4

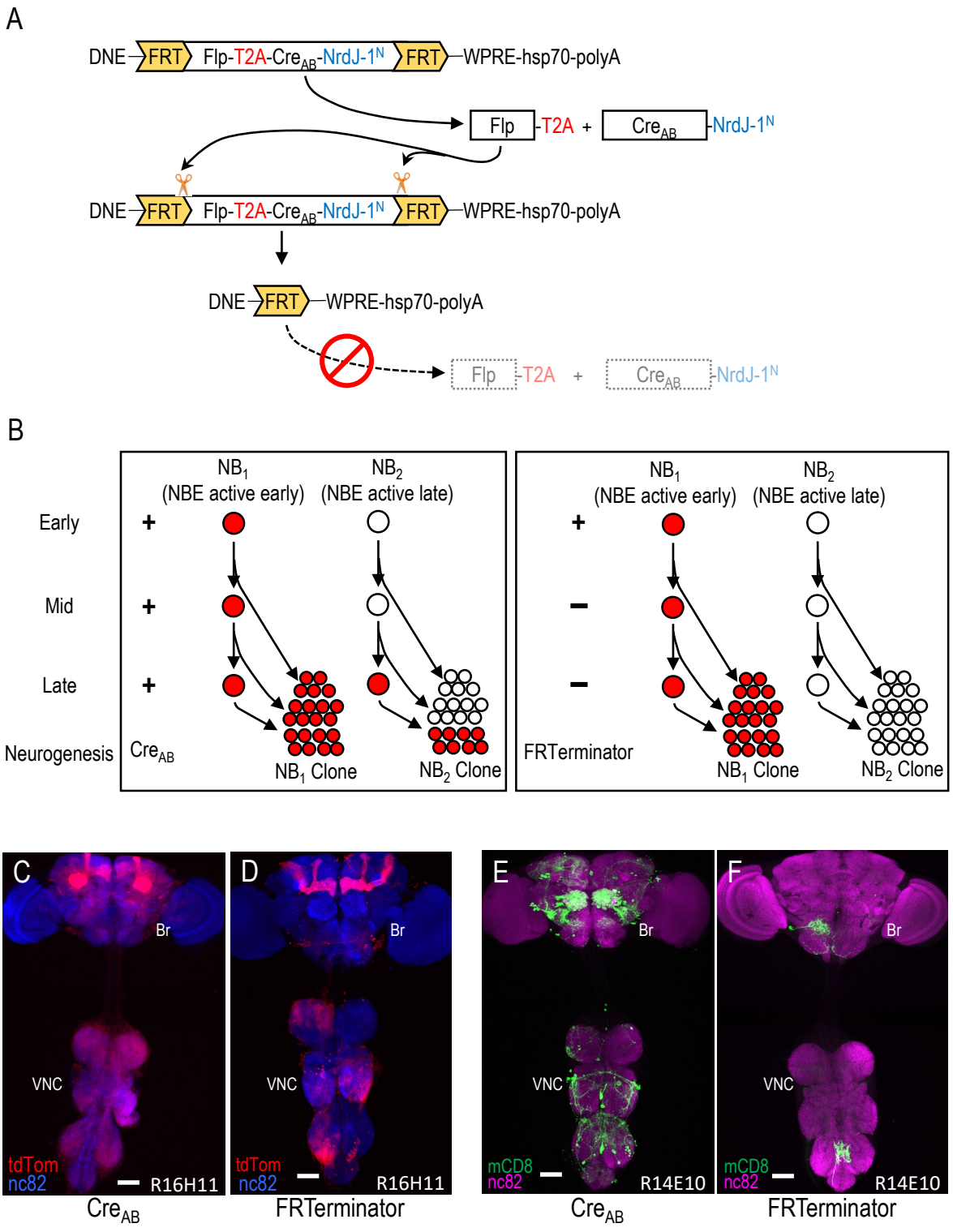
A
DNE
FRT
Flp-T2A-Cre$_{AB}$-NrdJ-1^{N}
FRT
WPRE-hsp70-polyA
Flp
-T2A +
Cre$_{AB}$
-NrdJ-1^{N}
B
NB$_1$
(NBE active early)
NB$_2$
(NBE active late)
Early
Mid
Late
Neurogenesis
Cre$_{AB}$
NB$_1$ Clone
NB$_2$ Clone
FRTerminator
C
D
E
F
Br
VNC
tdTom
nc82
R16H11
mCD8
R14E10
Cre$_{AB}$
FRTerminator